

# Identification of new Galactic symbiotic stars with SALT - II. New discoveries and characterization of the sample<sup>★</sup>

J. Merc,<sup>1,2</sup>  J. Mikołajewska,<sup>3</sup>  K. Ilkiewicz,<sup>3</sup>  B. Monard,<sup>4</sup>  A. Udalski<sup>5</sup> 

<sup>1</sup>*Astronomical Institute, Faculty of Mathematics and Physics, Charles University, V Holešovičkách 2, 180 00 Prague, Czech Republic*

<sup>2</sup>*Instituto de Astrofísica de Canarias, Calle Vía Láctea, s/n, E-38205 La Laguna, Tenerife, Spain*

<sup>3</sup>*Nicolaus Copernicus Astronomical Center, Polish Academy of Sciences, Bartycka 18, 00–716 Warsaw, Poland*

<sup>4</sup>*Kleinkaroo Observatory, Sint Helena 1B, PO Box 281, Calitzdorp 6660, South Africa*

<sup>5</sup>*Astronomical Observatory, University of Warsaw, Al. Ujazdowskie 4, 00–478 Warszawa, Poland*

Accepted 2025 December 01. Received 2025 December 01; in original form 2025 October 16

## ABSTRACT

We present the continuation of a systematic search for new southern Galactic symbiotic stars, selecting candidates from the SuperCOSMOS H $\alpha$  Survey and 2MASS. Follow-up spectroscopy with the Southern African Large Telescope (SALT) was used to confirm their symbiotic nature and to characterize the cool and hot components of the full sample, including systems from earlier work. We report 14 newly confirmed bona fide symbiotic stars and identify 6 additional strong candidates. Photometric variability was examined using our data and archival light curves from multiple all-sky surveys. Most systems are variable, with the majority showing periodic modulation consistent with orbital motion or pulsations. Possible photometric orbital periods are reported for 19 confirmed and 3 candidate systems, pending spectroscopic confirmation. Eight objects exhibit signs of outburst activity. In one of the systems, multiple brightenings occur at similar orbital phases, closely resembling the evolution of FN Sgr, a symbiotic binary with a magnetic white dwarf. The peculiar variability of another symbiotic star is best explained by dust-obscuration events. These results expand the census of Galactic symbiotic stars.

**Key words:** surveys – binaries: symbiotic – techniques: photometric, spectroscopic

## 1 INTRODUCTION

Symbiotic stars, binaries consisting of a red giant and a hot companion (white dwarf or, rarely, a neutron star), are among the interacting systems with the longest orbital periods. They are ideal for studying phenomena occurring in a variety of astrophysical sources, that are not yet fully understood and well incorporated in the models of stellar evolution, such as mass transfer and accretion, thermonuclear outbursts, winds, or jets (see the reviews on symbiotic stars by Mikołajewska 2012, Munari 2019, and Merc 2025). Despite the targeted search for the Galactic symbiotic stars is one of the active directions of the current research (Merc & Mikołajewska 2024) as evidenced by numerous studies in recent years (see, e.g., Corradi et al. 2008, 2010; Miszalski et al. 2013; Miszalski & Mikołajewska 2014; Rodríguez-Flores et al. 2014; Munari et al. 2021; Akras et al. 2021; Akras 2023; Xu et al. 2024; Lucy et al. 2024; Chen et al. 2025; Zhao et al. 2025; Ball et al. 2025; Botello et al. 2025; Merc et al. 2025a), their currently known number (<300; Merc et al. 2019a,b, 2025b) is still significantly lower than any estimate of the population size presented in the literature (ranging from a few thousands to a few hundred thousands; Allen 1984; Kenyon et al. 1993; Magrini et al. 2003; Laversveiler et al. 2025).

Given that a large fraction of symbiotic stars show very strong

emission lines, one of the methods to select promising candidates is to employ large photometric surveys conducted in the H $\alpha$  filter. Several new discoveries were achieved thanks to the INT Photometric H $\alpha$  survey (IPHAS; Drew et al. 2005), see Corradi et al. (2008, 2010) and Rodríguez-Flores et al. (2014), and the AAO/UKST SuperCOSMOS H $\alpha$  Survey (SHS; Parker et al. 2005). In case of a later survey, Miszalski et al. (2013) studied a  $\sim 35$  deg<sup>2</sup> region towards the Galactic bulge, discovering 20 new symbiotic stars and another 15 candidates. Miszalski & Mikołajewska (2014, hereafter Paper I) used the SHS survey to search for new Galactic southern symbiotic stars. The spectroscopic follow-up using the Southern African Large Telescope (SALT) resulted in the discovery of 12 new and 3 possible symbiotic stars.

In this paper, we continue in the systematic survey presented in Paper I and present the follow-up of additional sources selected using the criteria discussed in Sect. 2 of Paper I based on the SHS H $\alpha$  data and 2MASS near-infrared observations (Skrutskie et al. 2006). In addition to presenting new discoveries, we analyze some of the basic stellar parameters of the components of symbiotic stars from our sample (new and the ones from Paper I), study the variability of the stars, and, if possible, discuss their orbital parameters and pulsational properties of their cool components.

The paper is organized as follows: Section 2 describes the spectroscopic data and archival photometry used in this work. Section 3 presents the discovery of 14 new symbiotic stars and 6 strong candidates. In Section 4, we analyze the parameters of the symbiotic components in the full SALT sample, while Section 5 discusses their

<sup>★</sup> Based on observations made with the Southern African Large Telescope (SALT).

<sup>†</sup> E-mail: jaroslav.merc@mff.cuni.cz

**Table 1.** Log of SALT/RSS observations. Only the exposure times of longer exposures are given (see text).

Name (2MASS J)	Date (dd-mm-yy)	Exposure (s)
06503882-0006394	09-11-2013	1200
10532463-6044518	19-12-2013	1200
12283699-6519204	15-01-2014	1200
14031865-5809349	08-04-2022	462
16284838-4010161	01-05-2014	1170
16472941-3612388	02-05-2014	1170
16592100-4517173	14-05-2014	1170
17160302-3322285	01-05-2014	1170
17210951-4416404	13-06-2014	1800
17303001-3049372	13-07-2014	1170
17341102-3850446	14-07-2014	1170
17370406-3324539	14-05-2014	1170
17370603-2500098	22-06-2014	1170
17371139-3350500	21-05-2014	1170
17374702-2501120	11-08-2014	1170
17435611-2506254	12-06-2015	1200
17505978-3012473	29-06-2014	1170
17562573-1631486	16-06-2014	790
18002542-1126324	11-05-2014	1170
18075073-2516427	24-05-2015	1200
18155753-0837357	11-05-2014	1170

photometric variability with the aim of identifying orbital and pulsational periods. Section 6 focuses on individual noteworthy objects, and Section 7 summarizes our findings.

## 2 OBSERVATIONAL DATA

### 2.1 Optical spectroscopy

The new symbiotic candidates were observed spectroscopically using the Robert Stobie Spectrograph (RSS; [Burgh et al. 2003](#); [Kobulnicky et al. 2003](#)) on the SALT telescope ([Buckley et al. 2006](#); [O’Donoghue et al. 2006](#)) under programmes 2013-2-RSA\_POL-001 (PI: Miszalski), 2014-1-RSA\_POL-001 (PI: Miszalski), 2015-1-SCI-011 (PI: Miszalski), and 2021-2-SCI-009 (PI: Mikołajewska). The SALT/RSS spectra for symbiotic stars whose discovery was presented in [Paper I](#) were obtained under programme 2013-1-RSA\_POL-001 (PI: Miszalski). The details on the RSS configuration and processing of the spectra can be found in Section 3 of [Paper I](#). The log of new spectroscopic observations is listed in Tab. 1 and shows the 2MASS identification of the object, observing date, and exposure time of the longer of two exposures of the same star that was always taken after a short 30 or 60s exposure to measure H $\alpha$  unsaturated. The same information for symbiotic stars from [Paper I](#) that are also analyzed in this work is not repeated here, as it is presented in table 1 of the aforementioned paper.

### 2.2 Photometry

To study the variability of the target stars, we have searched for available data from the All-Sky Automated Survey for Supernovae (ASAS-SN; [Shappee et al. 2014](#); [Kochanek et al. 2017](#)), the Optical Gravitational Lensing Experiment survey (OGLE III and IV; [Udalski et al. 2008, 2015](#)), the Zwicky Transient Facility survey (ZTF; [Masci et al. 2019](#)), and the Asteroid Terrestrial-impact Last Alert System (ATLAS) project ([Tonry et al. 2018](#); [Smith et al. 2020](#)) obtained from the ATLAS Forced Photometry server ([Shingles et al. 2021](#)).

We have also searched for detections of the sources on the digitized photographic plates from the Harvard College Observatory from the DASCH (Digital Access to a Sky Century at Harvard) archive ([Laycock et al. 2010](#)). For some objects from [Paper I](#), we have also collected our photometry in the *V* and *I* filters using the 35 cm Schmidt–Cassegrain and Ritchey–Chretien telescopes equipped with SBIG CCD cameras at the Kleinkaroo Observatory in South Africa.

To search for periodicities in the light curves, we performed period analysis on individual datasets using the Lomb–Scargle method ([Lomb 1976](#); [Scargle 1982](#)), as well as the multi-band Lomb–Scargle variant ([VanderPlas & Ivezić 2015](#)), both implemented in the *astropy* Python package ([Astropy Collaboration et al. 2013, 2018, 2022](#)).

## 3 NEW SYMBIOTIC STARS

In this work, we present the discovery of 14 new symbiotic stars, and we also discuss 6 strong symbiotic candidates (see Table 2). To classify an object as a symbiotic star, we adopted the criteria of [Belczyński et al. \(2000\)](#) and [Miszalski et al. \(2013\)](#), namely we required the simultaneous presence of the late-type giant features in the spectrum (e.g., TiO, Ca II and other absorption lines) and detection of strong emission lines of H I and He I, together with emission lines with ionization potential of at least 35 eV (e.g., [O III], He II). The detection of Raman-scattered O VI lines at 6825 and 7082 Å ([Schmid 1989](#)) is a sufficient but not necessary condition for the symbiotic classification. These lines are observed in about half of the confirmed symbiotic systems (e.g., [Akras et al. 2019](#); [Merc et al. 2019a](#)).

The SALT spectra of new symbiotic stars are shown in Fig. 1. All of the newly discovered symbiotic stars show strong emission lines of H I and He I, and also of He II, [Fe VII], and nine of them show also Raman-scattered O VI lines. They are very intense in 2MASS J17371139-3350500. Two of the new bona-fide symbiotic stars were previously classified as H $\alpha$  emission sources by [Kohoutek & Wehmeyer \(2003\)](#), namely 2MASS J17370603-2500098 ([KW2003] 40) and 2MASS J17505978-3012473 ([KW2003] 69).

SALT spectra of the candidates are shown in Fig. 2. The optical spectra do not fully fulfill the criteria for definitive symbiotic classification (either due to the lack of highly ionized emission lines in the spectra or not definitive evidence for the red giant in the optical spectra). Several of the current symbiotic candidates were considered as possible PNe in the literature previously: 2MASS J06503882-0006394 was classified as a possible PN in [Vioque et al. \(2020\)](#), 2MASS J10532463-6044518 was classified as an H $\alpha$  emission line star by [Wray \(1966\)](#) and [Schwartz et al. \(1990\)](#), and as possible PN by [Vioque et al. \(2020\)](#). 2MASS J12283699-6519204 was previously classified as a likely PN by [Wray \(1966\)](#). However, the red 2MASS colors of these three candidates with PN-like spectra (marked D? in Table 3) are typical for D-type symbiotic stars and not for PNe. Furthermore, the approximate positions of the two D-type candidates, 2MASS J10532463-6044518 and J12283699-6519204, in the [O III] diagnostic diagram<sup>1</sup> ([Gutiérrez-Moreno et al. 1995](#); [Iłkiewicz & Mikołajewska 2017](#)) support a symbiotic rather than PN classification. No H $\gamma$  or [O III]  $\lambda$ 363 emission is detectable in 2MASS J06503882-0006394, and therefore this diagnostic cannot be applied to that object.

<sup>1</sup> The flux in the H $\gamma$  line could not be directly measured from the SALT spectra, as it lies near the blue edge of the spectral range; however, an approximate flux was derived from the red wing of the line.

**Table 2.** The list of the new and possible symbiotic stars detected in this work. Note that if the SIMBAD identifier is the same as the 2MASS name of the star, we do not repeat it in whole. The parallax ( $\varpi$ ) is from *Gaia* DR3 (Gaia Collaboration et al. 2023). The distances listed in the table are photogeometric distances from Bailer-Jones et al. (2021).

Name (2MASS J)	SIMBAD name	<i>Gaia</i> DR3	OGLE IV	$\ell$ ( $^{\circ}$ )	$b$ ( $^{\circ}$ )	$\varpi$ (mas)	d (kpc)
<i>Bona-fide</i>							
16284838-4010161	2MASS J162..	6017140952831727616	GD2159.10.14478	341.5504	5.8712	0.07 $\pm$ 0.03	6.6
16472941-3612388	2MASS J164..	6019738480355216512	-	346.9756	5.7579	-0.01 $\pm$ 0.02	9.1
17160302-3322285	Terz V 4021	5979017105159069312	BLG918.21.90	352.8160	2.8452	-0.02 $\pm$ 0.05	7.4
17303001-3049372	IRAS 17272-3047	4058383390530172288	BLG662.03.62513	356.6487	1.7567	0.56 $\pm$ 0.26	4.4
17341102-3850446	2MASS J173..	5961813076738022144	BLG674.19.27171	350.3400	-3.2534	0.02 $\pm$ 0.08	6.1
17370603-2500098	2MASS J173..	4062231784311861376	-	2.3399	3.6885	0.00 $\pm$ 0.07	6.8
17371139-3350500	2MASS J173..	4053683351942447104	-	354.8806	-1.0702	0.12 $\pm$ 0.14	6.2
17374702-2501120	2MASS J173..	4062219066862909952	BLG714.25.14317	2.4080	3.5484	0.12 $\pm$ 0.06	6.3
17435611-2506254	2MASS J174..	4067943811590065536	BLG633.07.22889	3.0705	2.3194	0.32 $\pm$ 0.07	4.2
17505978-3012473	MSX6C G359.5102-01.6611	4056361899741275392	BLG501.05.167800	359.5094	-1.6603	0.16 $\pm$ 0.08	6.8
17562573-1631486	IRAS 17535-1631	4144709995465485696	BLG837.03.36067	11.9486	4.1915	0.19 $\pm$ 0.04	3.9
18002542-1126324	ZTF J180025.42-112632.5	4151813325933260672	BLG840.30.24	16.8707	5.8606	-0.01 $\pm$ 0.04	8.3
18075073-2516427	OGLE BLG-LPV-214983	4065672156232576640	BLG580.22.74954	5.6472	-2.4394	-0.02 $\pm$ 0.07	6.4
18155753-0837357	2MASS J181..	4157938533401345920	-	21.1922	3.8577	0.05 $\pm$ 0.14	6.4
<i>Possible</i>							
06503882-0006394	IRAS 06480-0003	3113251991344790144	GD1730.11.5882	212.9406	-0.2265	0.25 $\pm$ 0.08	3.1
10532463-6044518	WRAY 15-678	5338200425455290368	GD1369.18.25889	289.0028	-1.1085	0.00 $\pm$ 0.06	6.3
12283699-6519204	WRAY 16-113	5860998619435294080	GD1304.13.26309	300.5507	-2.5562	0.48 $\pm$ 0.04	1.9
16592100-4517173	2MASS J165..	5964068591723229184	GD1082.31.90	341.3460	-1.7121	-0.04 $\pm$ 0.07	5.7
17210951-4416404	2MASS J172..	5953276610229325056	BLG987.08.13	344.4560	-4.2310	0.10 $\pm$ 0.03	5.6
17370406-3324539	2MASS J173..	4053748429286984320	BLG661.25.39044	355.2317	-0.8168	0.04 $\pm$ 0.14	6.9

**Table 3.** *Gaia* DR3 and 2MASS near-IR magnitudes of new and possible symbiotic stars detected in this work, together with the adopted value of interstellar extinction (see the text for details), infrared symbiotic type, spectral type of the giant, and the effective temperature obtained from the calibration of van Belle et al. (1999).

Name	$G_{BP}$ (mag)	$G$ (mag)	$G_{RP}$ (mag)	$J$ (mag)	$H$ (mag)	$K_s$ (mag)	$E_{(B-V)}$ (mag)	IR type	Giant SpT	$T_{eff}$ (K)
<i>Bona-fide</i>										
16284..	16.7	15.2	13.9	11.38	10.27	9.72	1.1	S	M1	3804
16472..	15.8	14.0	12.7	10.46	9.33	8.98	1.0	S	M3	3586
17160..	16.8	14.9	13.5	9.50	8.04	7.34	1.6	S	M0	3914
17303..	18.7	17.4	15.9	12.32	10.29	8.47	1.6	D	-	-
17341..	18.3	15.0	13.4	10.10	8.78	8.27	1.5	S	M5	3367
17370..	18.1	15.5	14.0	10.11	8.65	8.00	1.4	S	M2	3695
17371..	19.1	16.2	14.5	10.20	8.87	8.09	1.8	S	M0	3914
17374..	18.5	15.7	14.1	10.65	9.30	8.72	1.6	S	M3	3586
17435..	19.3	15.9	14.3	10.44	9.07	8.37	1.4	S	M3	3586
17505..	17.8	15.1	13.5	9.73	8.43	7.80	1.2	S	M2.5	3641
17562..	15.2	13.2	11.8	8.72	7.53	6.95	0.9	S	M4	3476
18002..	17.0	15.1	13.9	11.31	10.23	9.83	0.9	S	M2	3695
18075..	18.7	15.8	14.3	11.30	10.02	9.52	1.1	S	M3	3586
18155..	17.9	15.4	13.8	9.99	8.56	7.81	1.4	S	M2	3695
<i>Possible</i>										
06503..	17.5	16.8	16.0	13.60	11.95	10.56	0.5	D?	-	-
10532..	17.3	16.8	15.8	13.38	11.17	9.26	2.0	D?	-	-
12283..	14.8	14.6	13.5	12.18	10.90	9.65	0.3	D?	-	-
16592..	18.6	15.5	14.0	10.37	8.96	8.40	1.5	S?	M2	3695
17210..	16.8	14.5	13.1	10.39	9.16	8.71	1.1	S?	M4	3476
17370..	20.2	17.1	15.5	11.13	9.62	8.87	2.1	S?	-	-

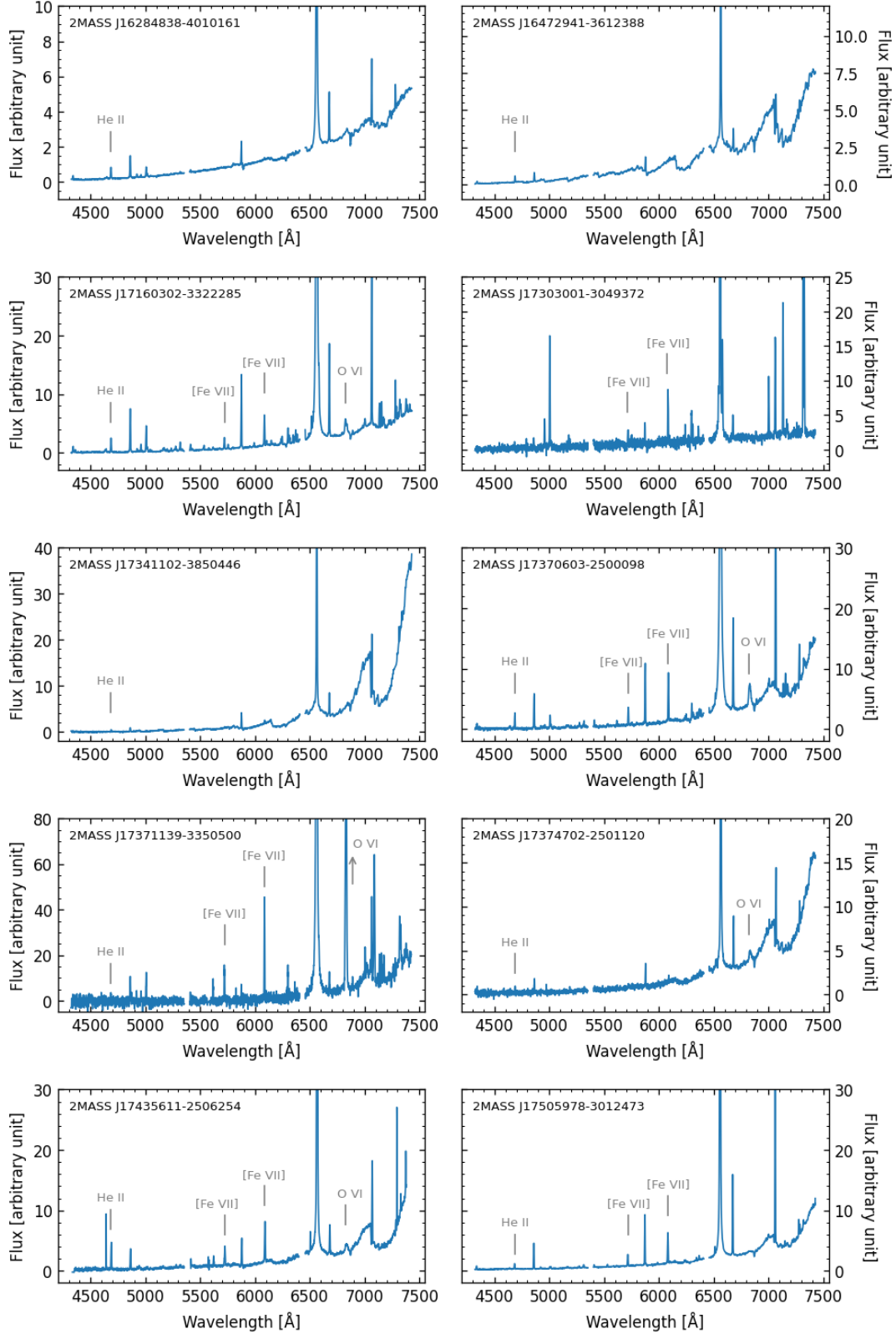


**Figure 1.** SALT/RSS spectra of new symbiotic stars. The spectra are not dereddened, and due to limitations in absolute flux calibration due to the moving pupil design of SALT, they are normalized by the average continuum value measured in the region 6 200–6 300 Å (see Miszalski & Mikolajewska 2014). The identification of selected emission lines is shown in gray. Most of the unmarked emission lines are of H I and He I.

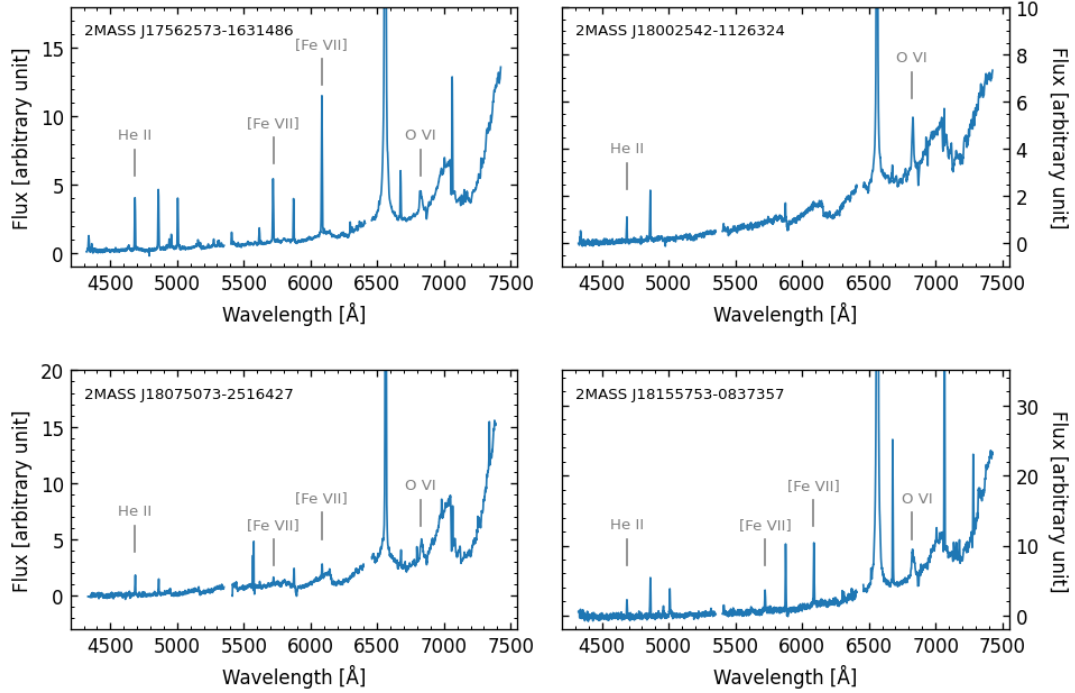


Figure 1 – continued SALT/RSS spectra of new symbiotic stars.

#### 4 STELLAR PARAMETERS OF THE SALT SAMPLE

All but one of the new symbiotic stars are classified as infrared type S ("stellar"; see Table 3, which also lists 2MASS magnitudes of target stars), with the red giant's presence clearly visible in our optical spectra (Fig. 1). 2MASS J17303001-3049372 exhibits the typical optical spectrum of a D-type symbiotic star, showing, for example, much stronger [O III]/H I ratios and prominent [N II] emission, features not typically seen in S-types (see, e.g., [Iłkiewicz & Mikołajewska 2017](#)). This classification is further supported by the infrared excess in its SED, characteristic of D-type symbiotics.

To estimate the spectral types of the cool companions in new S-type symbiotic stars and candidates, we adopted the same methodology as in [Paper I](#) and [Miszalski et al. \(2013\)](#), which utilizes the TiO indices from [Kenyon & Fernandez-Castro \(1987\)](#); see their equations 1 and 2. The resulting spectral types are provided in Table 3, and the corresponding effective temperatures were derived using the calibration by [van Belle et al. \(1999\)](#). Similar information for symbiotic stars from [Paper I](#) is available in Table A2. It should be noted that the optical spectral types represent upper limits, as the depths of the TiO bands are likely diluted by the blue (predominantly nebular) continuum. Near-infrared spectra of symbiotic stars typically indicate later spectral types, and for the same reason, the effective temperatures derived from the optical spectra should also be regarded as upper limits.

We have not estimated the luminosities of these symbiotic giants, as the distances to these objects remain uncertain. Table 2 lists photogeometric distances from [Bailer-Jones et al. \(2021\)](#), based on *Gaia* EDR3/DR3 data. However, for these distant symbiotic systems, the parallaxes are unreliable, with many being negative, despite RUWE values or goodness-of-fit statistics from *Gaia* appearing reasonable in some cases.

The hot components are typically not directly visible in the optical spectra of symbiotic systems but are evidenced by highly ionized

emission lines. These emission lines, influenced by the radiation of the hot component, provide indirect means to estimate its parameters.

The lower limit of the hot component's temperature is determined by the maximum ionization potential observed in the spectrum (see Table 4) and the relation  $T [10^3 \text{ K}] \sim IP_{\text{max}} [\text{eV}]$  proposed by [Murset & Nussbaumer \(1994\)](#). For the newly discovered symbiotic stars, the emission lines with maximum ionization potential are [Fe VII] or Raman-scattered O VI lines, implying hot component temperatures exceeding 99 kK or 114 kK, respectively. The same holds for symbiotic stars from [Paper I](#) (see Table A3), except for 2MASS J17334728-2719266, which only shows He II.

The temperature of the ionizing photon source, assuming case B recombination, can also be derived following the method of [Iijima \(1981\)](#), which involves fluxes of He I  $\lambda 4471$ , He II  $\lambda 4868$ , and H $\beta$  emission lines. These temperatures are provided in Tables 4 and A3. For most of the new symbiotic stars, the He I  $\lambda 4471$  flux is negligible (or very low and difficult to precisely measure due to the low S/N in the blue region), so it was neglected in the calculations, as done by [Sokoloski et al. \(2006\)](#) for Z And, and [Leedj  r   et al. \(2016\)](#) and [Merc et al. \(2017\)](#) for AG Dra.

Tables 4 and A3 list the fluxes of He II  $\lambda 4868$  and H $\beta$  lines, along with other prominent lines detected in the spectra. These fluxes were dereddened using the reddening values from Tables 2 and A1, respectively, assuming the [Cardelli et al. \(1989\)](#) reddening law and adopting a total-to-selective absorption ratio  $R = 3.1$ . The adopted reddening values correspond to the total reddening in the direction of the target stars at their distances, obtained using the `mw dust` code ([Bovy et al. 2016](#)) from combined 3D dust maps of [Drimmel et al. \(2003\)](#), [Marshall et al. \(2006\)](#), and [Green et al. \(2019\)](#).

The luminosity of the hot component can also be evaluated from optical emission lines (e.g., equation 8 of [Kenyon et al., 1991](#), and equations 6 and 7 of [Mikołajewska et al., 1997](#)). However, since the SALT spectra analyzed in this work are only relative, this approach is not applicable here.



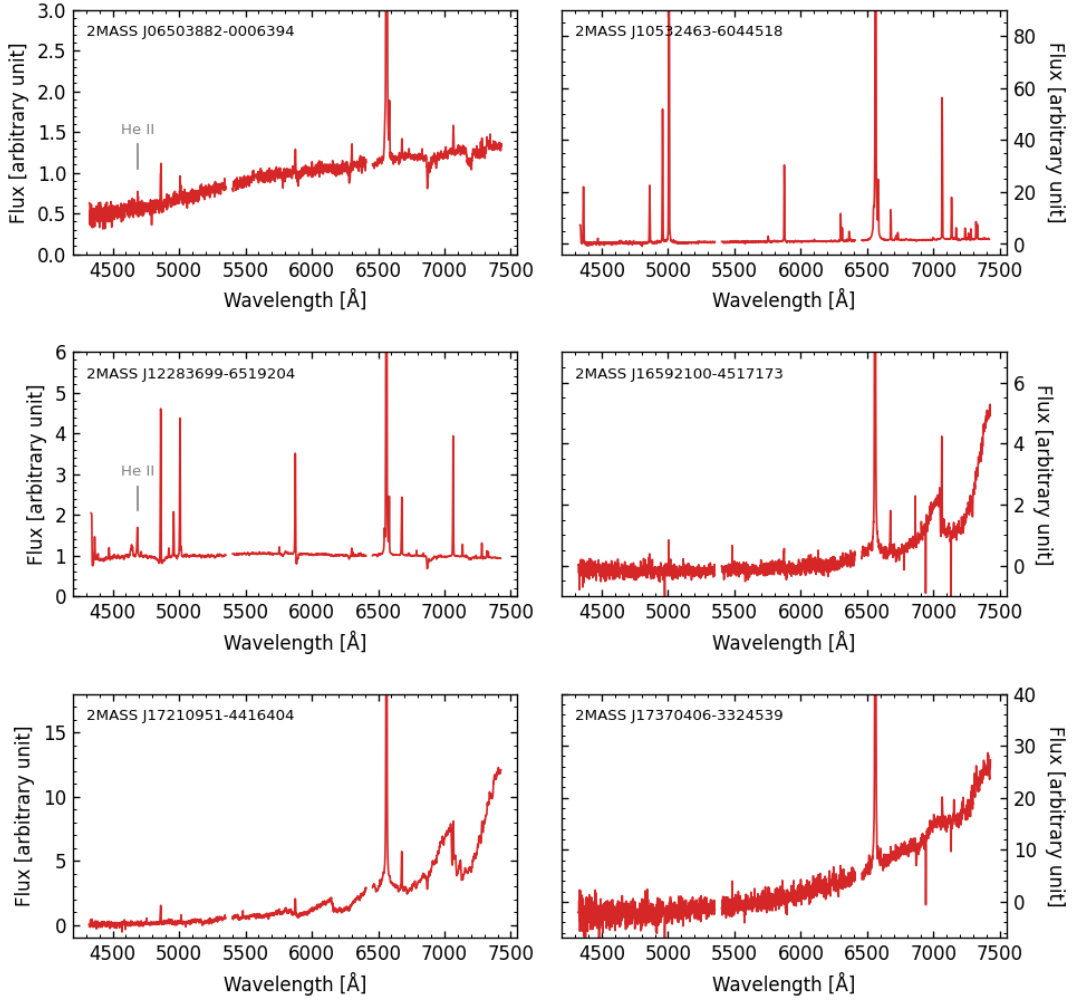


**Figure 2.** SALT/RSS spectra of possible symbiotic stars.

## 5 PHOTOMETRIC VARIABILITY

To study the variability of newly confirmed and candidate symbiotic stars identified in this work and in [Paper I](#), we compiled photometric data from various surveys. A large fraction of the objects have useful light curves available from the ATLAS survey<sup>2</sup>, and several are also covered by OGLE-IV, although in some cases the light curves are too short to allow reliable period analysis. Only a handful of sources have ASAS-SN data of sufficient quality, largely because most of the SALT sample is relatively faint and/or located in crowded fields. On the other hand, ZTF data are generally quite useful; however, the survey only observes objects with declinations above  $-30^\circ$ , which excludes a significant portion of the sample.

Light curves of bona-fide and candidate symbiotic stars from this work are presented in Fig. B1 and Fig. B2, respectively. The same information for objects from [Paper I](#) is shown in Fig. B3 and Fig. B4. With the exception of a few candidate symbiotic stars, all objects exhibit variability on some timescale, which is clearly periodic in most cases. Most of these systems are already classified as long-period variables or candidates in the literature, largely thanks to the

*Gaia* DR3 variability data (see [Lebzelter et al. 2023](#); [Rimoldini et al. 2023](#); [Eyer et al. 2023](#)). A summary of the main results of our analysis is provided below, while individual noteworthy systems are discussed in Sect. 6.

Tables 5 and A4 list the periodicities detected in the objects from this work and from [Paper I](#), respectively. In many cases, the dominant periodic signal is interpreted as the orbital period of the binary system, based on the characteristic timescales, amplitudes, color variations, and light-curve morphology (see more detailed discussion for individual objects in Sect. 6). In total, we identify tentative orbital periods for 19 bona-fide and 3 candidate symbiotic stars, ranging from 384 to 1518 days, a range typical for S-type symbiotic systems (e.g., [Gromadzki et al. 2013](#)). We emphasize that these values require confirmation through spectroscopic monitoring. Several light curves also show hints of eclipses.

In addition, possible pulsations of the cool component were detected in some cases, particularly after subtracting the orbital signal and/or in the redder bands. In four objects, the dominant variability appears to arise from Mira pulsations of the cool component. Among them, 2MASS J17303001-3049372 (this work) and 2MASS J16422739-4133105 ([Paper I](#)) are the only two confirmed D-type symbiotic stars in our combined sample. The other two, 2MASS J17371139-3350500 (this work) and 2MASS J17334728-

<sup>2</sup> Note that the data were obtained in non-standard filters: orange ( $\sim 5582\text{--}8249\text{ Å}$ ,  $\lambda_{\text{eff}} = 6630\text{ Å}$ ) and cyan ( $\sim 4157\text{--}6556\text{ Å}$ ,  $\lambda_{\text{eff}} = 5182\text{ Å}$ ).

**Table 4.** Fluxes of emission lines in the spectra of new and possible symbiotic stars relative to the flux of H $\beta$  line, together with the ion with the maximum ionization potential and the estimates of the hot component temperature.

Name	H $\gamma$ 4340 Å	[O III] 4363 Å	He II 4686 Å	H $\beta$ 4861 Å	[O III] 5007 Å	[Fe VII] 5721 Å	He I 5876 Å	[Fe VII] 6086 Å	H $\alpha$ 6563 Å	He I 6678 Å	O VI 6825 Å	He I 7065 Å	Ion	T $^a_h$ (10 <sup>3</sup> K)	T $^b_h$ (10 <sup>3</sup> K)
<i>Bona-fide</i>															
16284..	27	0	55	100	30	0	38	2	1414	61	20	53	O <sup>+5</sup>	114	156
16472..	30	7	72	100	0	6	71	6	1235	94	0	116	Fe <sup>+6</sup> .	99	171
17160..	28	7	38	100	46	10	49	21	1043	35	19	74	O <sup>+5</sup>	114	138
17303..	23	7	40	100	1247	79	75	205	4583	59	0	198	Fe <sup>+6</sup>	99	141
17341..	-	0	55	100	18	8	126	19	2101	119	0	225	Fe <sup>+6</sup> .	99	156
17370..	25	8	48	100	30	22	61	46	2896	58	40	116	O <sup>+5</sup>	114	149
17371..	-	0	23	100	95	47	17	125	5266	18	453	44	O <sup>+5</sup>	114	119
17374..	-	0	74	100	0	9	54	8	1727	70	47	71	O <sup>+5</sup>	114	173
17435..	-	4	155	100	5	47	47	75	1415	31	30	63	O <sup>+5</sup>	114	227
17505..	24	0	26	100	6	24	79	52	2571	82	0	143	Fe <sup>+6</sup>	99	123
17562..	32	14	96	100	69	60	32	114	2026	27	36	50	O <sup>+5</sup>	114	190
18002..	19	0	50	100	0	0	16	3	1692	15	88	19	O <sup>+5</sup>	114	151
18075..	-	0	151	100	0	24	58	40	2031	43	123	73	O <sup>+5</sup>	114	225
18155..	-	0	44	100	59	26	64	63	3526	84	54	148	O <sup>+5</sup>	114	145
<i>Possible</i>															
06503..	0	0	0	100	57	0	37	0	1757	26	0	33	O <sup>+2</sup>	35	-
10532..	-	273	0	100	564	0	31	0	718	6	0	20	O <sup>+2</sup>	35	-
12283..	-	22	28	100	88	0	51	0	791	28	0	51	He <sup>+2</sup>	54	127
16592..	-	0	0	100	150	0	84	0	6635	184	0	288	O <sup>+2</sup>	35	-
17210..	23	0	0	100	0	0	32	0	1172	73	0	55	He <sup>+1</sup>	25	-
17370..	-	0	0	100	0	0	2	0	450	2	0	6	He <sup>+1</sup>	25	-

**Notes.** <sup>a</sup>Temperature of the hot component estimated from the maximum ionization potential observed in the optical spectrum. <sup>b</sup>Temperature of the hot component estimated using the method of Iijima (1981). For further details, see the main text.

2719266 (Paper I), exhibit characteristics consistent with S-type systems. While none of the D-type candidates from either study show clear Mira-like pulsations, most are only covered by OGLE-IV; only 2MASS J06503882-0006394 has additional data from ATLAS and ZTF, and it shows complex variability.

Finally, eight of the confirmed symbiotic stars display signatures of outburst activity in their light curves. Seven of these were identified from modern survey data, while in one case, the outburst was detected on historical DASCH photographic plates.

## 6 INDIVIDUAL OBJECTS

In this section, we summarize the information on the noteworthy objects from the SALT sample.

### 6.1 Bona-fide symbiotics

#### 2MASS J14031865-5809349

Prior to its confirmation as an S-type symbiotic binary in Paper I, this object was long known as an emission-line star (Wray 1966). Its quiescent spectrum reveals the presence of an M4 giant and a tentative detection of [Fe VII], along with strong He II emission lines.

An outburst of this object was detected by the *Gaia* satellite and reported as Gaia22bou on April 12, 2022 (Hodgkin et al. 2022), through the *Gaia* Science Alerts (GSA) pipeline (Hodgkin et al. 2021). The outburst is clearly visible in our data, ASAS-SN and ATLAS photometric data (see Fig. B3), and it is evident that the system had already been in an active state for several months prior to the alert. The *Gaia* G-band light curve, available from the GSA website and shown in Fig. 3, reveals that the main outburst was

**Table 5.** Variability of new and possible symbiotic stars.

Name	P <sub>orb</sub> (days)	P <sub>pul</sub> (days)	P <sub>other</sub> (days)	Outbursts	Eclipses
<i>Bona-fide</i>					
16284..	741				
16472..	502:	81:	901:		
17160..	1518:	142		Yes	
17303..		548			
17341..	694:				
17370..	778				
17371..		253			
17374..	435:			Yes	
17435..	667 <sup>a</sup>			Yes	
17505..		43.4, 49.1	934		Yes?
17562..	1339	88:			
18002..	792	35	408:	Yes <sup>b</sup>	
18075..	791	61		Yes	Yes:?
18155..	890		472, 81:	Yes	
<i>Possible</i>					
06503..					
10532..					
12283..			409:		
16592..			444::		
17210..	506	33			
17370..	785:			Yes?	Yes:?

**Notes.** <sup>a</sup>Value derived from the minima rather than from the period analysis, which yields a slightly longer period of 701 days. <sup>b</sup>Detected on the DASCH photographic plates; see the text for further details.

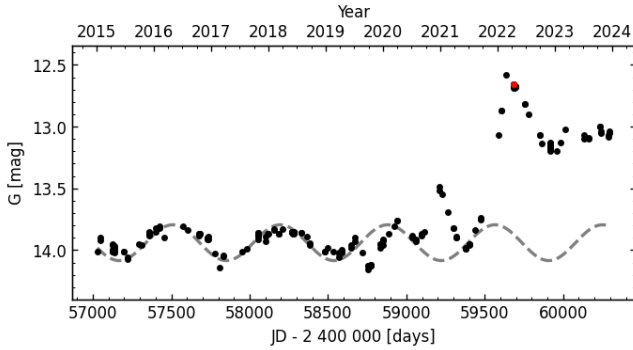


**Figure 3.** *Gaia* *G*-band light curve of 2MASS J14031865-5809349. The time of the issued *Gaia* Science Alert is marked with a red symbol. The underlying quiescent sinusoidal variability, with a period of 685 days, is shown in gray (see text for details).

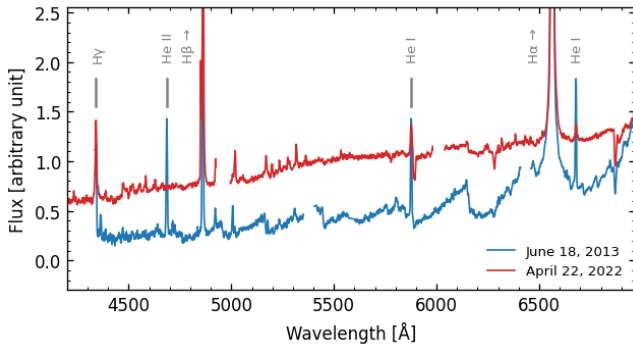


**Figure 4.** Comparison of the quiescent (blue) and outburst (red) spectra of 2MASS J14031865-5809349, obtained with SALT. Selected emission lines are identified in gray. Most of the remaining, unmarked emission features, particularly in the outburst spectrum, are due to Fe II.

preceded by a smaller brightening of approximately 0.5 mag in *G*, peaking around December 2020 (JD 2 459 210). This earlier event is also visible in our data (in particular in the *I* filter), but is hidden in the noise in the ASAS-SN *g*-band data. Furthermore, pre-outburst activity likely began between July and September 2019, with the variability of the system deviating from the previously observed sinusoidal pattern, in particular well visible in *Gaia* light curve.

The period of the quiescent variability is  $\sim 685$  days (inferred from the *Gaia* *G* light curve, but consistent with our *V* data—see the maxima in the light curve in Fig. B3 around JD 2 457 500 and JD 2 458 200), which we interpret as the orbital period of the binary. While other datasets suggest a possible period of 563 days (see Table A4), this shorter period is likely related to the morphology of the outburst phase (several maxima repeated with timescale close to this value) rather than orbital motion.

Our data in the *V* and *I* filters indicate an outburst amplitude of around 2.5 and 1.0 mag, respectively. An amplitude of about 1.5 mag is observed in the broader *Gaia* *G*-band. Several later rebrightenings are apparent in our data as well as the ASAS-SN and ATLAS light curves, and such photometric behaviour is typical of classical symbiotic star outbursts.

Following the *Gaia* alert, two low-resolution spectra were obtained on April 18 and 20, 2022 (JD 2 459 687.9 and JD

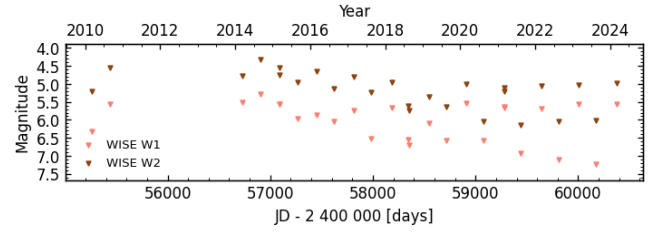


**Figure 5.** AllWISE and NEOWISE W1 and W2-band light curves of 2MASS J16422739-4133105.

2 459 689.7), and analyzed by Merc et al. (2022b), who concluded that the star was undergoing a classical Z And-type outburst, the first ever recorded for this system. During the outburst, high-ionization lines such as He II and [Fe VII] disappeared from the spectra. We obtained an additional outburst spectrum with SALT on April 22, 2022 (JD 2 459 691.5). A comparison of the quiescent and outburst spectra is shown in Fig. 4. These data confirm a drop in the ionization temperature of the hot component: high-ionization lines such as [Fe VII], He II, and [O III] are absent, while numerous Fe II lines emerge during outburst. Simultaneously, a rise in the blue continuum veiled the molecular bands of the cool companion.

#### 2MASS J16422739-4133105

The optical spectrum presented in Paper I allowed this target to be classified as a D-type symbiotic star, showing a rich emission-line spectrum, including Raman-scattered O VI lines. The OGLE-IV, ATLAS, and our own data reveal large-amplitude variability with a period of about 369 days (Fig. B3), consistent with a Mira pulsator, as expected for a D-type symbiotic system. The variability amplitude, however, appears to be strongly variable. Significant changes in amplitude (up to  $\sim 1.5$  mag) are also present in the mid-IR photometry from the Wide-field Infrared Survey Explorer (WISE; Wright et al. 2010), both in the AllWISE release and in the NEOWISE measurements (Mainzer et al. 2011, 2014), see Fig. 5. Owing to the  $\sim 6$ -month cadence of NEOWISE and the variability period being close to one year, it is difficult to trace amplitude variations in detail. Nonetheless, the data suggest that when the system was slightly brighter in the mid-IR, both the optical and mid-IR amplitudes were smaller, likely related to dust production by the Mira and the resulting increased extinction.

#### 2MASS J17160302-3322285

The variability of this newly confirmed S-type symbiotic star was first reported by Terzan et al. (1997), where it is listed as Terz V 4021 with an R-band magnitude between 15.8 and 17.6 mag. ATLAS *c*- and *o*-band data span about 3400 days and show clear variability (Fig. B1); however, period analysis is highly uncertain, particularly due to three distinct brightenings observed around JD 2 458 360, 2 459 750, and 2 460 800. The first two events had amplitudes of about 0.5 mag in *o*, while the third reached roughly 1.0 mag in *o* and 1.5 mag in *c*. These amplitudes should be treated with caution, as the star lies in a relatively crowded field. OGLE-IV data suggest a shorter period of about 142 days, which we interpret as due to pulsations of the giant.

#### 2MASS J17334728-2719266

This star was classified as an S-type symbiotic system with an M2 giant donor and a typical symbiotic spectrum, including emission lines up to He II, in Paper I. While analyzing its variability here, we



noticed a peculiar beating pattern and recovered two close periods of 161 and 179 days (Fig. B3). Given the intriguing nature of this variability, we carried out a more detailed analysis, combining these data with additional infrared spectroscopy and imaging, and presented the results separately in [Merc et al. \(2025c\)](#). The main conclusion of that study is that the beating pattern in the light curve is caused by the presence of two pulsating stars in close proximity. Moreover, the original identification of the symbiotic star was incorrect: it had been associated with the wrong *Gaia* source. The object now confirmed as the symbiotic star exhibits a pulsation period of 161 days.

### 2MASS J17374702-2501120

This star is classified here as a new S-type symbiotic system with an M3 cool component, exhibiting highly ionized emission lines such as He II, [Fe VII], and O VI.

In the photometric data (see Fig. B1), we identified several outbursts. Two brightenings are clearly visible in the OGLE-IV light curve, with maxima in April 2015 (JD 2457 115) and June 2016 (JD 2457 550), each reaching an amplitude of about 1 mag in the *I* band. The second event is also detected in the ATLAS data, with a similar amplitude of  $\sim 1$  mag in the *o* band. Two additional outbursts are captured by ATLAS: one in August 2017 (JD 2457 975) with amplitudes of 2 mag in *o* and 2.8 mag in *c*, and a less prominent one in July 2020 (JD 2459 050), with amplitudes of about 1 mag in *o* and 1.5 mag in *c*. The latter was also detected by ZTF. The recurrence timescale, amplitude, and duration of these events suggest that they are classical Z And-type symbiotic outbursts. No further outbursts have been observed since then.

Given the data quality, we used only the pre-outburst OGLE observations to determine the variability period, which we estimate to be approximately 435 days. We interpret this as the orbital period of the system.

### 2MASS J17391715-3546593

[Miszalski & Mikołajewska \(2014\)](#) classified this object as an S-type symbiotic system, with a typical spectrum showing highly ionized emission lines, such as [Fe VII] and O VI, superimposed on the continuum of an early M-type giant. Previously, it had been considered a PN following its discovery by [Kohoutek \(1994\)](#).

While the spectrum is not unusual for a symbiotic star, the photometric evolution is highly peculiar (Fig. 6). The OGLE-IV *I*-band light curve reveals a sharp brightening of at least 2.5 mag in 2010–2011, followed by five years of gradual decline accompanied by low-amplitude variability with a  $\sim 153$ -day period. In 2016, the brightness dropped relatively abruptly, but OGLE coverage resumed only in 2023 with a single point consistent with another high state. This gap is well covered by ATLAS, which recorded the system in a low state and then documented the onset of a second high state in 2018–2019. Although a direct comparison between the two high states is not possible due to differences in photometric systems, a rough estimate suggests the brightening recurred after about  $\sim 3\,200$  days, with the most recent high state showing a similar slow decline that is now slightly longer than the previous one.

Part of the pre-2010 low state is covered by mid-IR photometry from WISE in the AllWISE release, while subsequent *W1* and *W2* measurements from the NEOWISE mission span the first high state, the following low state, and the second high state. The mid-IR light curves broadly mirror the optical behavior.

The color evolution is interesting. In the ATLAS optical bands (*c*–*o*), the source became bluer during the optical minimum, whereas in the mid-IR (*W1*–*W2*) it became redder. Such behavior is inconsis-

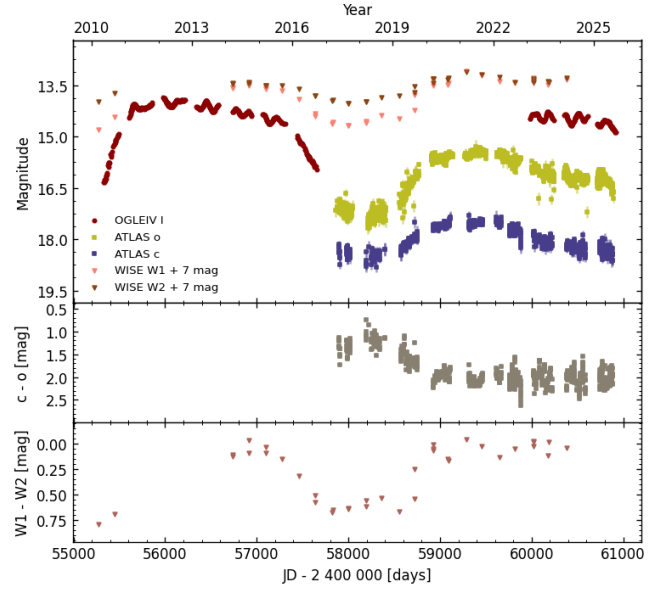


**Figure 6.** Photometric evolution of 2MASS J17391715-3546593 over the past  $\sim 16$  years. The upper panel shows the OGLE, ATLAS, and WISE light curves of the object. The middle panel displays the ATLAS *c* – *o* color evolution, while the bottom panel shows the WISE *W1* – *W2* color evolution.

tent with simple orbital variability (the amplitude-color dependence does not match) and is also unlike typical outburst activity, where the star becomes bluer as it brightens.

A more plausible explanation is a dust-obscuration event in which direct light from the cool giant is attenuated while the emission from the nebula and/or hot component remains largely unaffected, leading to a bluer optical color. The reddening of the mid-IR SED could result either from the appearance of a warm dust component peaking more strongly in *W2* than in *W1*, or from suppression of the cooler stellar continuum while the other components of the system contribute little at these wavelengths.

A similar behavior has been reported in other symbiotic systems, particularly those hosting Mira donors. The best-studied case is RX Pup ([Mikołajewska et al. 1999](#), see also Sect. 3 of [Mikołajewska 2000](#)). Analogous evolution is also well known in R CrB stars (e.g., [Clayton 1996](#); [Crawford et al. 2025](#)), and a comparable mechanism has been invoked to explain the “Great Dimming” of Betelgeuse in 2019–2020 (e.g., [Kravchenko et al. 2021](#); [Dupree et al. 2022](#); [Jadlovský et al. 2024](#)).

### 2MASS J17435611-2506254

Photometric data of this newly confirmed S-type symbiotic system show periodic variability with a period of 660 days, with a light curve morphology reminiscent of eclipses (Fig. B1). In addition to this variability, at least four outbursts with an amplitude  $> 0.5$  mag in *I*-band are clearly visible in the OGLE-IV light curve: in September 2010 ( $\sim$ JD 2 455 460), February 2014 (JD 2 456 710), February 2016 (JD 2 457 440), and August 2017 (JD 2 457 980; with the decline missing due to a seasonal gap). The last event is also covered by ATLAS data.

The phased light curve (Fig. 7) indicates that all brightening events occur at a similar orbital phase. Its overall shape closely resembles that of FN Sgr, a symbiotic system hosting a magnetic white dwarf ([Magdolen et al. 2023](#)). In that case, the most plausible explanation

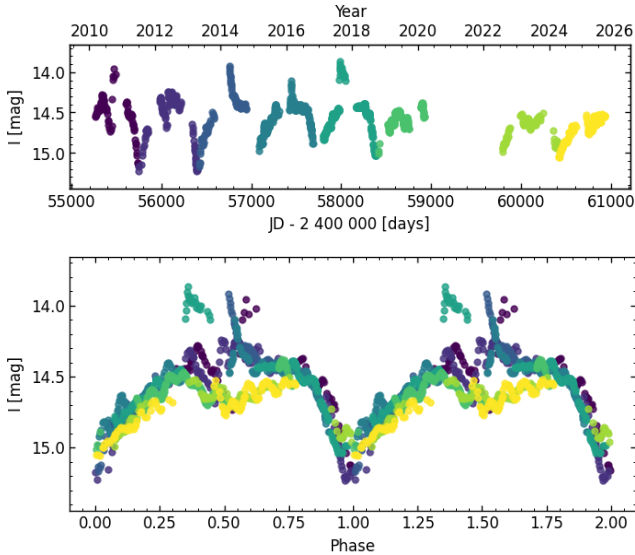


**Figure 7.** OGLE-IV *I*-band light curve of 2MASS J17435611-2506254. The upper panel shows the full light curve, color-coded by cycle, the lower panel displays the phased light curve using the same color scheme.

involved enhanced visibility of the stream–disc overflow. Notably, in at least three cycles of 2MASS J17435611-2506254, a secondary dip around phase 0.4–0.5 mag is also present. This feature further strengthens the analogy with FN Sgr, where similar minima have been attributed to ellipsoidal variability.

### 2MASS J17505978-3012473

Only OGLE photometry is available for this newly classified S-type symbiotic system. The light curve exhibits peculiar deep, eclipse-like minima. Folding the OGLE-IV data yields a very clean periodicity of 934 days, with the deep minima recurring at a consistent phase during that part of the survey. However, the deep minimum seen in the earlier OGLE-III light curve does not fall at the same phase when extrapolated with this period (it occurred about 130 days later than expected; phase shift of 0.14).

The stars in the vicinity of 2MASS J17505978-3012473 do not exhibit comparable variations, making it unlikely that the observed behavior is an artifact. Even disregarding the sudden change in periodicity, the amplitude of variability (noting that OGLE data are obtained in the *I* band) is too large to be explained by eclipses in symbiotic systems. Deep eclipses are typically observed only during outbursts, when the hot companion dominates the optical flux and the red giant contributes minimally (see, for example, CI Cyg, Kenyon et al. 1991; V618 Sgr, Merc et al. 2023; Hen 3-860, Merc et al. 2022a; or PU Vul, Kato et al. 2011). This is clearly not the case here, as the SALT spectrum obtained in 2014 shows both the clear signature of the red giant and the presence of highly ionized emission lines, typical for quiescent spectra of symbiotics (Fig. 1). The unusually deep features in the light curve therefore remain without a satisfactory explanation and warrant further investigation.

In addition to the long-term variability, the system also displays short-term variations, most likely attributable to pulsations of the cool component. Period analysis of the OGLE-IV light curve reveals two significant periodicities (after prewhitening the data to remove the dominant periodic signal), at approximately 43 and 49 days, while

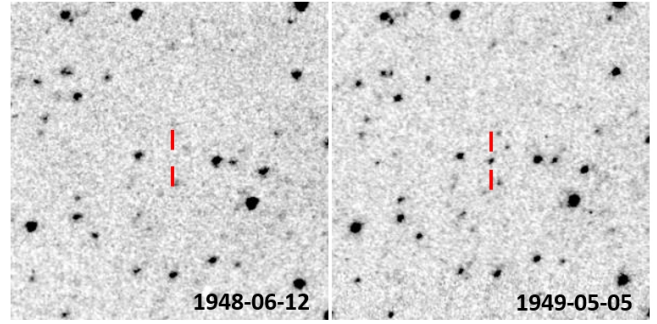


**Figure 8.** Two DASCH plates obtained before and during the 1949 outburst of 2MASS J18002542-1126324.

the OGLE-III data show evidence only for the longer of these periods.

### 2MASS J18002542-1126324

This newly discovered S-type symbiotic system was previously classified as a semi-regular variable with a period of 250 days based on ZTF data (Chen et al. 2020). However, our analysis shows that this is a yearly alias of a longer, 792-day period, which is consistently present across all datasets (Fig. B1).

Furthermore, our analysis revealed that the star underwent an outburst in 1949, which has not been previously reported in the literature but is clearly visible in DASCH plate data (Fig. 8). The star is distinctly detected on 11 plates taken between May 3 and June 15, 1949, with magnitudes between 15.0 and 15.4. Following this, only a few plates from 1950–1951 have limiting magnitudes around 16. Most plates taken until 1953 have limiting magnitudes between 9 and 13. A gap in observations exists between 1953 and 1964. All plates from 1964 onward have limiting magnitudes between 10.0 and 15.0, fainter than the maximum brightness reached during the 1949 event. Notably, pre-outburst plates show no detection of the star down to a limiting magnitude of  $\sim 17.5$ . The last such deep plate with a limiting magnitude greater than 15 mag was obtained in July 1948. Given the limited information, it is difficult to determine the nature of the outburst, whether it was a classical Z And-type symbiotic outburst or an eruption of a slow symbiotic nova.

### 2MASS J18075073-2516427

This newly confirmed S-type symbiotic star, with an M3 cool component and a relatively hot companion, as evidenced by the presence of O VI lines in the optical spectrum, experienced an outburst in June 2023 (around JD 2 460 100), clearly visible in ZTF data (Fig. B1). The event had an amplitude of approximately 1.1 mag in the *r* band and 1.5 mag in the *g* band, and is also detectable in the ATLAS light curve. Another, even more prominent outburst, seen in the ATLAS and OGLE-IV data, peaked around March 2025 (JD 2 460 750). Its amplitude was at least 1.5–2.0 mag in the ATLAS filters and 0.6 mag in *I* band; however, the quiescent magnitude in the ATLAS filters is not well constrained owing to the noisy data. The observed evolution, duration, and recurrence timescale of these events are consistent with classical symbiotic outbursts. Finally, we note that the OGLE quiescent light curve reveals regular eclipse-like minima with a period of  $\sim 786$  days, broadly consistent with the results of the period analysis.

### 2MASS J18155753-0837357

This is another newly confirmed S-type symbiotic star. Its photometric behavior is complex, with a recent outburst clearly visible in the

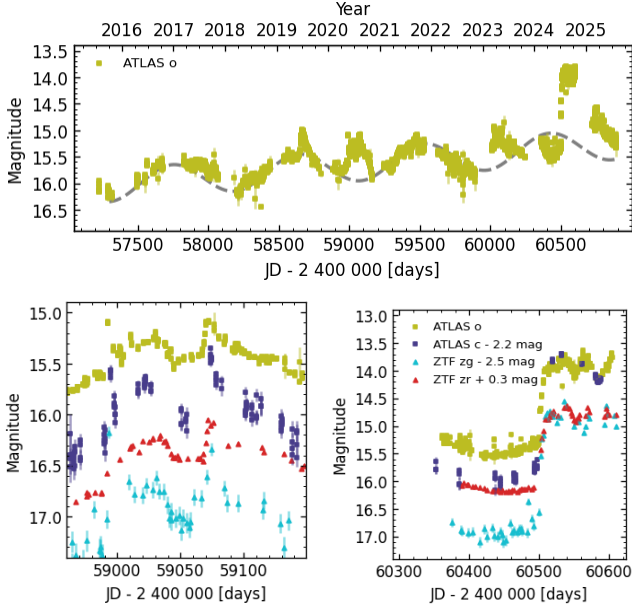


**Figure 9.** Variability of 2MASS J18155753-0837357. The upper panel shows the ATLAS *o*-band light curve, fitted with a sinusoidal curve with a period of 890 days combined with a linear trend. The lower panels present details of the 2020 outburst and the outburst that has been ongoing since July 2024.

ATLAS and ZTF light curves. Period analysis of the pre-outburst data suggested a period of about 472 days (Fig. B1 and Table 5); however, this appears to be linked to additional activity rather than the orbital motion of the system. The light curve is more consistently modulated with a period of 890 days and shows a rising trend over the observed interval (Fig. 9), which may correspond to the orbital period.

Interestingly, the brightening that occurred around the minimum of the presumed sinusoidal variation in 2020 appears to have been abruptly "interrupted" for about 35 days (around JD 2 459 050). ZTF data suggest that the system became redder during this interval. Such a color change would be consistent with an eclipse of the hot component in a symbiotic system; however, the available data are insufficient to search for additional similar events. A comparable interruption of an outburst was observed in Gaia18aen (Merc et al. 2020), where the source likewise reddened. Nevertheless, establishing a firm connection with orbital motion requires spectroscopic orbital data. Finally, we also note that part of the ATLAS *c* light curve (between JD 2 459 650 and 2 459 860) shows hints of an 81-day period, which is, however, not detectable in other datasets.

## 6.2 Possible symbiotic stars

### 2MASS J06503882-0006394

The absence of molecular bands in the spectrum, combined with the near-IR colors, suggests that this star is a possible D-type symbiotic system. It is listed as a semiregular variable with a period of  $\sim 346$  days in Chen et al. (2020). The ATLAS and ZTF light curves (Fig. B2) reveal complex photometric variability with no clear periodicity, characterized by several relatively deep minima that are not evenly spaced in time. If the object is indeed a D-type symbiotic star, its orbital period would likely be on the order of decades, and

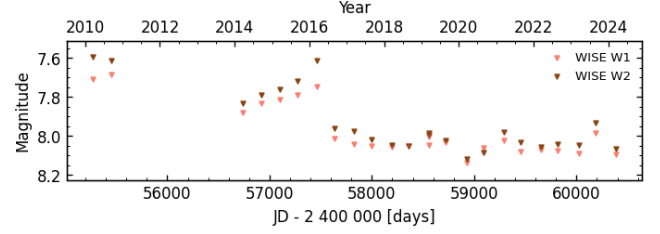


**Figure 10.** AllWISE and NEOWISE *W1* and *W2*-band light curves of 2MASS J17460199-3303085.

thus eclipses would not be expected to appear in the light curve.

### 2MASS J17370406-3324539

The SALT/RSS optical spectrum of this candidate with a relatively low signal-to-noise ratio shows only Balmer lines and He I (Fig. 2). The red part of the spectrum exhibits possible molecular band features, suggesting the presence of a red giant. The ASAS-SN light curve is noisy and reveals no significant periodic variability (Fig. B2). The OGLE-IV *I*-band data show a 0.3–0.4 mag increase in brightness at the beginning of the observed interval (JD < 2 457 000). Contemporaneous ASAS-SN *V*-band measurements display only a minor offset ( $\sim 0.1$  mag) from later observations, but the data quality is considerably lower. The *I*-band variability is consistent with a Z And-type outburst in a symbiotic system; however, the available data are insufficient to fully confirm this interpretation. Period analysis of the OGLE-IV light curve yields a period of  $\sim 785$  days, consistent with the minima in the data.

### 2MASS J17460199-3303085

The ATLAS photometry is noisy but indicates periodic variability with a period of about 719 days, whereas our data suggest a slightly longer period of  $\sim 775$  days (Fig. B4, Table A4). In addition to the periodic signal, our light curve clearly shows what appears to be a decline from an outburst of more than 2 mag in the *V* band. The same outburst is also visible in the NEOWISE *W1* and *W2* light curves, which exhibit a  $\sim 0.5$  mag brightening between 2014 and 2016 (Fig. 10). When combined with the AllWISE measurements in the same bands from 2010, the data suggest that the source maintained a comparable brightness level for at least six years, although possible dimming episodes between the AllWISE and NEOWISE epochs cannot be confirmed. Unfortunately, both our and the ATLAS data cover only the decline phase of this outburst.

We only have a lower limit on the amplitudes in the *V* and *I* bands, but they are consistent with typical Z And-type outbursts of symbiotic stars. The amplitudes in *W1* and *W2* are also in line with those observed during outbursts of other symbiotic systems (e.g., V390 Sco; Merc et al. 2024). The SALT spectrum used for the tentative symbiotic classification (Paper I) was obtained in September 2013. If the system was in outburst at that time, it could explain why the spectrum shows only low-ionization emission lines (Balmer lines of H I, He I, and faint [O III]). A quiescent spectrum could therefore provide a definitive confirmation of the symbiotic nature of this target.



## 7 CONCLUSIONS

In this work, we continued the systematic search for new Galactic southern symbiotic stars, selecting candidates from SHS and 2MASS data following the criteria of [Paper I](#). Spectroscopy obtained with SALT was used to confirm the symbiotic nature of the selected candidates and to characterize the components of the entire sample, including those from [Paper I](#).

We report the discovery of 14 new bona-fide symbiotic systems and 6 additional strong candidates. Of the newly confirmed systems, 13 are S-type with oxygen-rich M-type giants, and one is D-type. All show [Fe VII] and/or O VI emission lines in their optical spectra, with one system possibly also exhibiting [Fe X]. Among the candidates, three are likely D-type and three S-type.

We analyzed the photometric variability of the systems, confirming most as variables, with the majority showing periodic modulation attributable to orbital motion or pulsations. In total, we present possible (photometric) orbital periods for 19 bona-fide and 3 possible symbiotic stars. These periods should be confirmed through dedicated spectroscopic follow-up.

For 2MASS J17391715-3546593, the unusual photometric evolution is most likely caused by dust-obscuration events. Eight sources show evidence of outburst activity in their light curves. Notably, 2MASS J17435611-2506254 exhibits several brightenings occurring at similar orbital phases, closely resembling evolution of FN Sgr, symbiotic binary with magnetic white dwarf.

## ACKNOWLEDGEMENTS

We thank the anonymous referee for the careful review and helpful suggestions that improved the manuscript. The research of JaM was supported by the Czech Science Foundation (GACR) project no. 24-10608O. JMik was supported by the Polish National Science Centre (NCN) grant 2023/48/Q/ST9/00138. KI was supported by the Polish National Science Centre (NCN) grant 2024/55/D/ST9/01713. The OGLE project has received funding from the Polish National Science Centre grant OPUS-28 2024/55/B/ST9/00447 to AU. The paper is based on spectroscopic observations made with the Southern African Large Telescope (SALT). Polish participation in SALT is funded by grant No. MEiN 2021/WK/01.

## DATA AVAILABILITY

Our photometric data will be shared on reasonable request to the corresponding author. Additional photometric observations are accessible from the websites of the surveys. Spectra are available in the SALT archive.

## REFERENCES

- Akras S., 2023, *MNRAS*, **519**, 6044
- Akras S., Guzman-Ramirez L., Leal-Ferreira M. L., Ramos-Larios G., 2019, *ApJS*, **240**, 21
- Akras S., Gonçalves D. R., Alvarez-Candal A., Pereira C. B., 2021, *MNRAS*, **502**, 2513
- Allen D. A., 1984, *Publ. Astron. Soc. Australia*, **5**, 369
- Astropy Collaboration et al., 2013, *A&A*, **558**, A33
- Astropy Collaboration et al., 2018, *AJ*, **156**, 123
- Astropy Collaboration et al., 2022, *ApJ*, **935**, 167
- Bailer-Jones C. A. L., Rybizki J., Fouesneau M., Demleitner M., Andrae R., 2021, *AJ*, **161**, 147
- Ball S. E., Bromley B. C., Kenyon S. J., 2025, *arXiv e-prints*, p. [arXiv:2506.20505](#)
- Belczyński K., Mikołajewska J., Munari U., Ivison R. J., Friedjung M., 2000, *A&AS*, **146**, 407
- Botello M. K., Sabin L., Gómez-Muñoz M. A., 2025, *MNRAS*,
- Bovy J., Rix H.-W., Green G. M., Schlafly E. F., Finkbeiner D. P., 2016, *ApJ*, **818**, 130
- Buckley D. A. H., Swart G. P., Meiring J. G., 2006, in Stepp L. M., ed., Society of Photo-Optical Instrumentation Engineers (SPIE) Conference Series Vol. 6267, Ground-based and Airborne Telescopes. p. 62670Z, [doi:10.1117/12.673750](#)
- Burgh E. B., Nordsieck K. H., Kobulnicky H. A., Williams T. B., O'Donoghue D., Smith M. P., Percival J. W., 2003, in Iye M., Moorwood A. F. M., eds, Society of Photo-Optical Instrumentation Engineers (SPIE) Conference Series Vol. 4841, Instrument Design and Performance for Optical/Infrared Ground-based Telescopes. pp 1463–1471, [doi:10.1117/12.460312](#)
- Cardelli J. A., Clayton G. C., Mathis J. S., 1989, *ApJ*, **345**, 245
- Chen X., Wang S., Deng L., de Grijs R., Yang M., Tian H., 2020, *ApJS*, **249**, 18
- Chen J., Wang L., Li Y.-B., Ma X.-X., Luo A. L., Zhang Z.-C., Ding M.-Y., Zhang K., 2025, *ApJ*, **987**, 147
- Clayton G. C., 1996, *PASP*, **108**, 225
- Corradi R. L. M., et al., 2008, *A&A*, **480**, 409
- Corradi R. L. M., et al., 2010, *A&A*, **509**, A41
- Crawford C. L., Soon J., Clayton G. C., Tisserand P., Bedding T. R., Clark C. J., Lee C.-U., 2025, *MNRAS*, **537**, 2635
- Drew J. E., et al., 2005, *MNRAS*, **362**, 753
- Drimmel R., Cabrera-Lavers A., López-Corredoira M., 2003, *A&A*, **409**, 205
- Dupree A. K., et al., 2022, *ApJ*, **936**, 18
- Eyer L., et al., 2023, *A&A*, **674**, A13
- Gaia Collaboration et al., 2023, *A&A*, **674**, A1
- Green G. M., Schlafly E., Zucker C., Speagle J. S., Finkbeiner D., 2019, *ApJ*, **887**, 93
- Gromadzki M., Mikołajewska J., Soszyński I., 2013, *Acta Astron.*, **63**, 405
- Gutierrez-Moreno A., Moreno H., Cortes G., 1995, *PASP*, **107**, 462
- Hodgkin S. T., et al., 2021, *A&A*, **652**, A76
- Hodgkin S. T., et al., 2022, Transient Name Server Discovery Report, **2022-993**, 1
- Iijima T., 1981, in Photometric and Spectroscopic Binary Systems. p. 517, [doi:10.1007/978-94-009-8486-8\\_27](#)
- Ilkiewicz K., Mikołajewska J., 2017, *A&A*, **606**, A110
- Jadlovský D., et al., 2024, *A&A*, **685**, A124
- Kato M., Hachisu I., Cassatella A., González-Riestra R., 2011, *ApJ*, **727**, 72
- Kenyon S. J., Fernandez-Castro T., 1987, *AJ*, **93**, 938
- Kenyon S. J., Oliverson N. A., Mikołajewska J., Mikołajewski M., Stencel R. E., Garcia M. R., Anderson C. M., 1991, *AJ*, **101**, 637
- Kenyon S. J., Livio M., Mikołajewska J., Tout C. A., 1993, *ApJ*, **407**, L81
- Kobulnicky H. A., Nordsieck K. H., Burgh E. B., Smith M. P., Percival J. W., Williams T. B., O'Donoghue D., 2003, in Iye M., Moorwood A. F. M., eds, Society of Photo-Optical Instrumentation Engineers (SPIE) Conference Series Vol. 4841, Instrument Design and Performance for Optical/Infrared Ground-based Telescopes. pp 1634–1644, [doi:10.1117/12.460315](#)
- Kochanek C. S., et al., 2017, *PASP*, **129**, 104502
- Kohoutek L., 1994, *Astronomische Nachrichten*, **315**, 235
- Kohoutek L., Wehmeyer R., 2003, *Astronomische Nachrichten*, **324**, 437
- Kravchenko K., et al., 2021, *A&A*, **650**, L17
- Laversweiler M., Gonçalves D. R., Rocha-Pinto H. J., Merc J., 2025, *A&A*, **698**, A155
- Laycock S., Tang S., Grindlay J., Los E., Simcoe R., Mink D., 2010, *AJ*, **140**, 1062
- Lebzelter T., et al., 2023, *A&A*, **674**, A15
- Leedjävär L., Gális R., Hric L., Merc J., Burmeister M., 2016, *MNRAS*, **456**, 2558
- Lomb N. R., 1976, *Ap&SS*, **39**, 447
- Lucy A. B., et al., 2024, *arXiv e-prints*, p. [arXiv:2412.00855](#)

Magdolen J., Dobrotka A., Orio M., Mikołajewska J., Vanderburg A., Monard B., Aloisi R., Bezák P., 2023, *A&A*, **675**, A140

Magrini L., Corradi R. L. M., Munari U., 2003, in Corradi R. L. M., Mikołajewska J., Mahoney T. J., eds, *Astronomical Society of the Pacific Conference Series Vol. 303, Symbiotic Stars Probing Stellar Evolution*. p. 539 ([arXiv:astro-ph/0208085](#)), doi:10.48550/arXiv.astro-ph/0208085

Mainzer A., et al., 2011, *ApJ*, **731**, 53

Mainzer A., et al., 2014, *ApJ*, **792**, 30

Marshall D. J., Robin A. C., Reylé C., Schultheis M., Picaud S., 2006, *A&A*, **453**, 635

Masci F. J., et al., 2019, *PASP*, **131**, 018003

Merc J., 2025, *Galaxies*, **13**, 49

Merc J., Mikołajewska J., 2024, *Nature Astronomy*, **8**, 1504

Merc J., Gális R., Leedjäv L., 2017, in *The Golden Age of Cataclysmic Variables and Related Objects IV*. p. 60 ([arXiv:1806.05935](#)), doi:10.22323/1.315.0060

Merc J., Gális R., Wolf M., 2019a, *Research Notes of the American Astronomical Society*, **3**, 28

Merc J., Gális R., Wolf M., 2019b, *Astronomische Nachrichten*, **340**, 598

Merc J., et al., 2020, *A&A*, **644**, A49

Merc J., Gális R., Wolf M., Velez P., Bohlson T., Barlow B. N., 2022a, *MNRAS*, **510**, 1404

Merc J., et al., 2022b, *The Astronomer's Telegram*, **15340**, 1

Merc J., et al., 2023, *MNRAS*, **523**, 163

Merc J., Velez P., Charbonnel S., Garde O., Le Dû P., Mulato L., Petit T., Skowron J., 2024, *Astronomische Nachrichten*, **345**, e20240017

Merc J., Mulato L., Charbonnel S., Garde O., Le Dû P., Petit T., 2025a, in preparation

Merc J., Gális R., Wolf M., 2025b, submitted to *ApJS*

Merc J., Mikołajewska J., Gałan C., Ilkiewicz K., Beck P. G., Monard B., Gromadzki M., 2025c, *arXiv e-prints*, p. [arXiv:2511.22988](#)

Mikołajewska J., 2000, in Kastner J. H., Soker N., Rappaport S., eds, *Astronomical Society of the Pacific Conference Series Vol. 199, Asymmetrical Planetary Nebulae II: From Origins to Microstructures*. p. 431 ([arXiv:astro-ph/0001012](#)), doi:10.48550/arXiv.astro-ph/0001012

Mikołajewska J., 2012, *Baltic Astronomy*, **21**, 5

Mikołajewska J., Acker A., Stenholm B., 1997, *A&A*, **327**, 191

Mikołajewska J., Brandt E., Hack W., Whitelock P. A., Barba R., Garcia L., Marang F., 1999, *MNRAS*, **305**, 190

Miszalski B., Mikołajewska J., 2014, *MNRAS*, **440**, 1410

Miszalski B., Mikołajewska J., Udalski A., 2013, *MNRAS*, **432**, 3186

Munari U., 2019, *arXiv e-prints*, p. [arXiv:1909.01389](#)

Munari U., et al., 2021, *MNRAS*, **505**, 6121

Murset U., Nussbaumer H., 1994, *A&A*, **282**, 586

O'Donoghue D., et al., 2006, *MNRAS*, **372**, 151

Parker Q. A., et al., 2005, *MNRAS*, **362**, 689

Rimoldini L., et al., 2023, *A&A*, **674**, A14

Rodríguez-Flores E. R., Corradi R. L. M., Mampaso A., García-Alvarez D., Munari U., Greimel R., Rubio-Díez M. M., Santander-García M., 2014, *A&A*, **567**, A49

Scargle J. D., 1982, *ApJ*, **263**, 835

Schmid H. M., 1989, *A&A*, **211**, L31

Schwartz R. D., Persson S. E., Hamann F. W., 1990, *AJ*, **100**, 793

Shappee B. J., et al., 2014, *ApJ*, **788**, 48

Shingles L., et al., 2021, *Transient Name Server AstroNote*, **7**, 1

Skrutskie M. F., et al., 2006, *AJ*, **131**, 1163

Smith K. W., et al., 2020, *PASP*, **132**, 085002

Sokoloski J. L., et al., 2006, *ApJ*, **636**, 1002

Terzan A., Bernard A., Guibert J., 1997, *A&AS*, **123**, 507

Tonry J. L., et al., 2018, *PASP*, **130**, 064505

Udalski A., Szymanski M. K., Soszynski I., Poleski R., 2008, *Acta Astron.*, **58**, 69

Udalski A., Szymański M. K., Szymański G., 2015, *Acta Astron.*, **65**, 1

VanderPlas J. T., Ivezić Ž., 2015, *ApJ*, **812**, 18

Vioque M., Oudmaijer R. D., Schreiner M., Mendigutía I., Baines D., Mowlavi N., Pérez-Martínez R., 2020, *A&A*, **638**, A21

Wray J. D., 1966, PhD thesis, Northwestern University

Wright E. L., et al., 2010, *AJ*, **140**, 1868

Xu X.-j., Shao Y., Li X.-D., 2024, *ApJ*, **962**, 126

Zhao Y., Guo S., Lv G., Li J., Zhu C., Shi J., 2025, *arXiv e-prints*, p. [arXiv:2507.20206](#)

van Belle G. T., et al., 1999, *AJ*, **117**, 521

This paper has been typeset from a  $\text{\LaTeX}$  file prepared by the author.

## APPENDIX A: SYMBIOTIC STARS FROM PAPER I

The list of bona-fide and possible symbiotic stars from [Paper I](#), together with their SIMBAD and *Gaia* DR3 identifiers, galactic coordinates, parallaxes, distances and *Gaia* magnitudes is in Table [A1](#). Their SALT/RSS spectra are shown in figs. 1-4 of the aforementioned paper. The infrared 2MASS magnitudes, together with their infrared types, spectral types of the giants, and their effective temperatures are in Table [A2](#). The fluxes of emission lines and the temperatures of the hot components are listed in Table [A3](#). Information on their variability is in [A4](#).

## APPENDIX B: PHOTOMETRY

In this appendix, we present light curves and periodograms of all studied symbiotic stars and candidates. Figure [B1](#) shows data for the newly identified symbiotic stars from this work, while Fig. [B2](#) presents data for the new candidates. Symbiotic stars and candidates from [Paper I](#) are shown in Fig. [B3](#) and Fig. [B4](#), respectively.



**Table A1.** The list of the bona-fide and possible symbiotic stars from [Paper I](#). The columns are the same as in Table 2.

Name (2MASS J)	SIMBAD name	<i>Gaia</i> DR3	OGLE IV	$\ell$ ( $^{\circ}$ )	$b$ ( $^{\circ}$ )	$\varpi$ (mas)	d (kpc)
<i>Bona-fide</i>							
14031865-5809349	WRAY 15-1167	5871060800085618816	GD1247.27.6	312.3148	3.3967	0.09±0.02	7.0
15431767-5857221	2MASS J154..	5834224583611758592	GD1181.19.24296	323.5413	-3.1423	0.00±0.02	12.8
16003761-4835228	2MASS J160..	5984320908710818944	GD1152.19.59	332.0679	3.2823	0.08±0.03	6.1
16422739-4133105	IRAS 16389-4127	5968218384802364032	GD1102.09.592	342.2640	3.0318	0.00±0.07	7.8
17050868-4849122	2MASS J170..	5938619188187996800	GD1916.27.23710	339.1468	-4.6493	0.07±0.03	6.6
17334728-2719266	Terz V 2513	4061345440488592896*	BLG611.15.9091*	359.9792	3.0664	-0.29±0.13	6.7
17391715-3546593	PN K 5-8	4041216852950479616	BLG610.21.103715	353.4730	-2.4679	-0.17±0.14	10.1
17422035-2401162	OGLE BLG-LPV-19199	4068379669255286912	BLG626.18.75294	3.8061	3.1974	-0.04±0.05	8.3
17463311-2419558	2MASS J174..	4068133481744764032	BLG633.28.25	4.0423	2.2155	0.14±0.05	5.7
18131474-1007218	2MASS J181..	4157296551738802432	-	19.5540	3.7375	0.05±0.04	6.5
18272892-1555547	2MASS J182..	4097140453884745088	BLG576.15.38	16.0601	-2.0558	0.19±0.08	4.1
18300636-1940315	2MASS J183..	4092813080982916736	BLG579.11.85	13.0225	-4.3378	-0.08±0.04	9.7
<i>Possible</i>							
16503229-4742288	IRAS 16468-4737	5939392802025441152	GD1100.27.1204	338.5095	-2.0533	0.14±0.18	4.0
17145509-3933117	IRAS 17114-3929	5972229544962050432	BLG990.18.2562	347.6561	-0.5638	0.18±0.10	3.9
17460199-3303085	2MASS J174..	4053970672432264192	-	356.5300	-2.2173	0.04±0.03	7.7

**Notes.** \*Although another *Gaia* source (and OGLE source) lies closer to the 2MASS position, the analysis of [Merc et al. \(2025c\)](#) confirms that the source ID listed here corresponds to the symbiotic star. See the text for further details.

**Table A2.** *Gaia* DR3 magnitudes, 2MASS near-IR magnitudes, extinction, IR types, giant spectral types and effective temperatures of bona-fide and possible symbiotic stars from [Paper I](#). The columns are the same as in Table 3.

Name	$G_{BP}$ (mag)	$G$ (mag)	$G_{RP}$ (mag)	$J$ (mag)	$H$ (mag)	$K_s$ (mag)	$E_{(B-V)}$ (mag)	IR type	Giant SpT	$T_{eff}$ (K)
<i>Bona-fide</i>										
14031..	15.6	13.9	12.6	10.42	9.32	8.94	0.6	S	M4	3476
15431..	16.4	14.7	13.5	11.22	10.13	9.72	0.6	S	M2.5	3641
16003..	16.8	14.7	13.3	10.8	9.47	8.89	1.3	S	C-N5 C24.5	-
16422..	17.1	16.4	15.4	10.33	8.96	7.66	1.2	D	-	-
17050..	15.9	13.9	12.5	10.04	8.95	8.57	0.6	S	M4	3476
17334..	16.6	14.9	12.5	9.32	7.91	7.26	1.6	S	M2	3695
17391..	18.2	16.6	15.1	9.81	8.44	7.63	1.2	S	M1.5	3750
17422..	17.2	15.0	13.6	10.2	8.99	8.43	1.0	S	M2:	3695
17463..	17.6	15.1	13.6	9.86	8.51	7.91	1.3	S	M4:	3476
18131..	17.3	15.0	13.7	10.94	9.64	9.18	1.3	S	M0	3914
18272..	16.9	14.3	12.8	9.16	7.8	7.18	1.1	S	M1	3804
18300..	16.7	15.0	13.7	11.07	9.96	9.55	0.8	S	M3.5	3531
<i>Possible</i>										
16503..	19.4	18.5	17.4	13.99	11.55	9.48	1.5	D?	-	-
17145..	17.8	17.3	16.1	11.92	9.62	7.87	0.9	D?	-	-
17460..	16.4	14.7	13.3	9.86	8.7	8.17	1.4	S?	K5-M0	3969

**Table A3.** Fluxes of emission lines in the spectra of new and possible symbiotic stars from Paper I. The columns are the same as in Table 4.

Name	H $\gamma$ 4340 Å	[O III] 4363 Å	He II 4686 Å	H $\beta$ 4861 Å	[O III] 5007 Å	[Fe VII] 5721 Å	He I 5876 Å	[Fe VII] 6086 Å	H $\alpha$ 6563 Å	He I 6678 Å	O VI 6825 Å	He I 7065 Å	Ion	T <sub>h</sub> <sup>a</sup> (10 <sup>3</sup> K)	T <sub>h</sub> <sup>b</sup> (10 <sup>3</sup> K)
<i>Bona-fide</i>															
14031..	-	7	40	100	7	0	21	1	539	18	0	21	Fe <sup>+6</sup> :	99	141
15431..	30	0	83	100	0	11	14	16	780	28	77	10	O <sup>+5</sup>	114	180
16003..	22	0	56	100	0	9	16	0	928	13	80	20	O <sup>+5</sup>	114	157
16422..	39	29	73	100	144	27	9	48	477	3	20	8	O <sup>+5</sup>	114	172
17050..	-	3	28	100	3	2	20	4	562	21	5	20	O <sup>+5</sup>	114	126
17334..	-	53	12	100	119	0	34	0	638	12	0	31	He <sup>+2</sup>	54	100
17391..	-	7	62	100	16	24	21	41	945	9	15	20	O <sup>+5</sup>	114	163
17422..	-	0	51	100	17	10	24	15	761	16	6	20	O <sup>+5</sup>	114	152
17463..	-	4	73	100	58	28	48	52	971	19	0	51	Fe <sup>+6</sup>	99	172
18131..	-	6	38	100	4	1	30	0	606	40	12	30	O <sup>+5</sup>	114	139
18272..	-	0	43	100	0	4	39	7	1170	36	27	44	O <sup>+5</sup>	114	144
18300..	-	9	123	100	0	2	27	7	926	9	86	24	O <sup>+5</sup>	114	208
<i>Possible</i>															
16503..	-	107	0	100	759	0	58	0	1301	18	0	67	O <sup>+2</sup>	14	-
17145..	-	52	0	100	416	0	41	0	757	14	0	50	O <sup>+2</sup>	14	-
17460..	-	4	0	100	19	0	31	0	840	16	0	18	O <sup>+2</sup>	14	-

**Notes.** <sup>a</sup>Temperature of the hot component estimated from the maximum ionization potential observed in the optical spectrum. <sup>b</sup>Temperature of the hot component estimated using the method of Iijima (1981). For further details, see the main text.

**Table A4.** Variability of bona-fide and possible symbiotic stars from Paper I.

Name	P <sub>orb</sub> (days)	P <sub>pul</sub> (days)	P <sub>other</sub> (days)	Outbursts	Eclipses
<i>Bona-fide</i>					
14031..	685 <sup>a</sup>		563:	Yes	
15431..	592:	61			
16003..	388	51:			
16422..		369			
17050..	824: <sup>b</sup>				
17334..		161 <sup>c</sup>			
17391..		153	3200:		
17422..	1056	90			
17463..	968	52			
18131..	446				
18272..	1261				
18300..	1353	78	506		
<i>Possible</i>					
16503..			35 <sup>d</sup>		
17145..					
17460..	729				

**Notes.** <sup>a</sup>Orbital period inferred from *Gaia* *G*-band data available through the *Gaia* Science Alerts website (see Sect. 6 for details). <sup>b</sup>Comparison of the *V*- and *I*-band data suggests the presence of ellipsoidal variability, typically interpreted as due to a tidally distorted giant. At longer wavelengths, where the giant dominates the light (unlike shorter wavelengths dominated by the nebula and/or hot companion), two minima and maxima per orbital period are expected (see, e.g., Fig. 6.2 in Munari 2019). Consequently, we adopt twice the dominant period as the orbital period. <sup>c</sup>Value adopted from the analysis of Merc et al. (2025c), see text for further discussion. <sup>d</sup>If the object is indeed a D-type symbiotic system, the 35-day period detected in the OGLE-IV *I*-band data would be unusually short for the pulsation period of the cool Mira component.

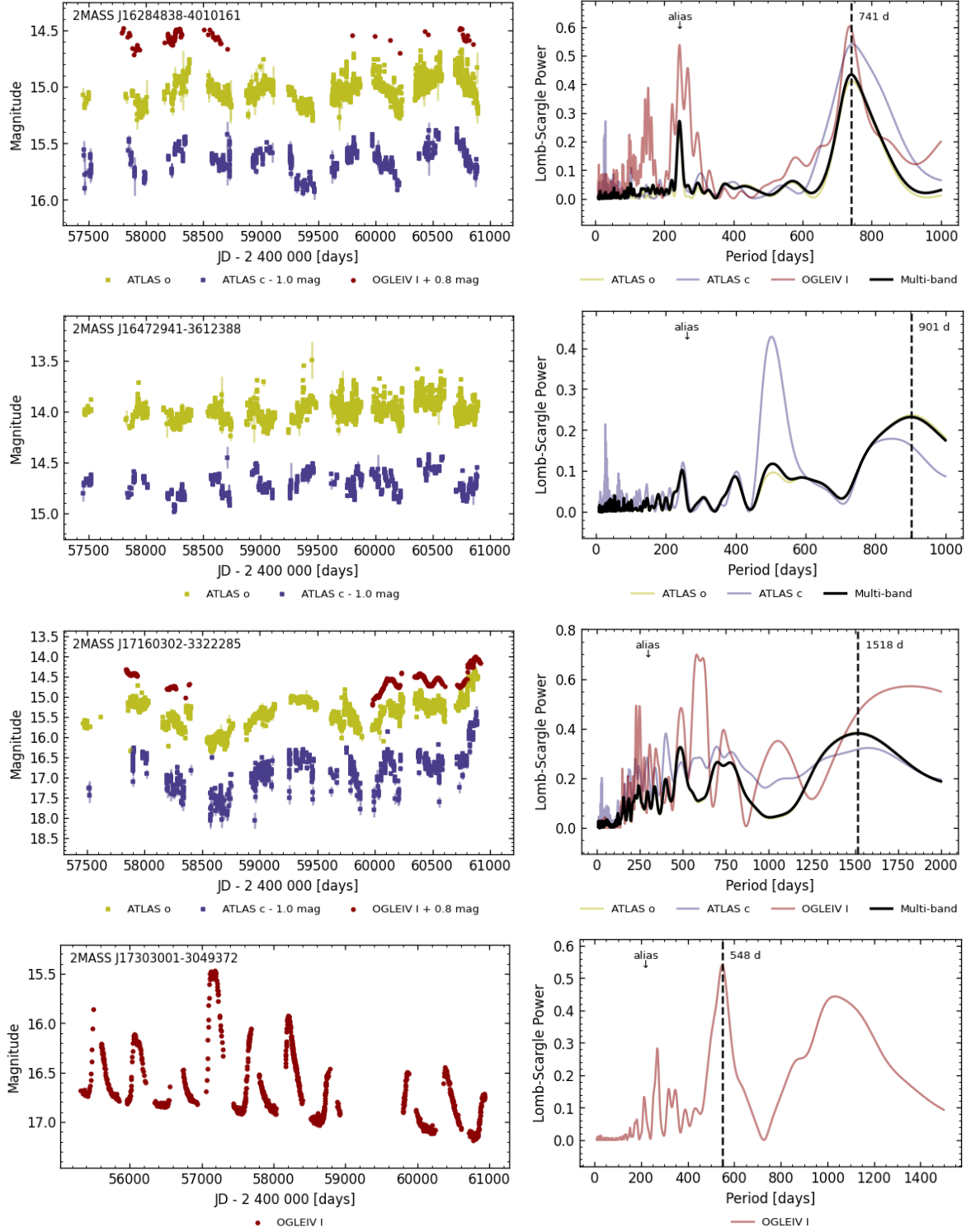


**Figure B1.** Light curves and Lomb–Scargle periodograms of the new symbiotic stars from this work. For visual clarity, some datasets are shifted by a constant value, as indicated in the legend of each panel. In the periodogram panels, the most prominent period, typically obtained from the multi-band analysis, is marked by a vertical dashed line, with its yearly aliases also indicated.

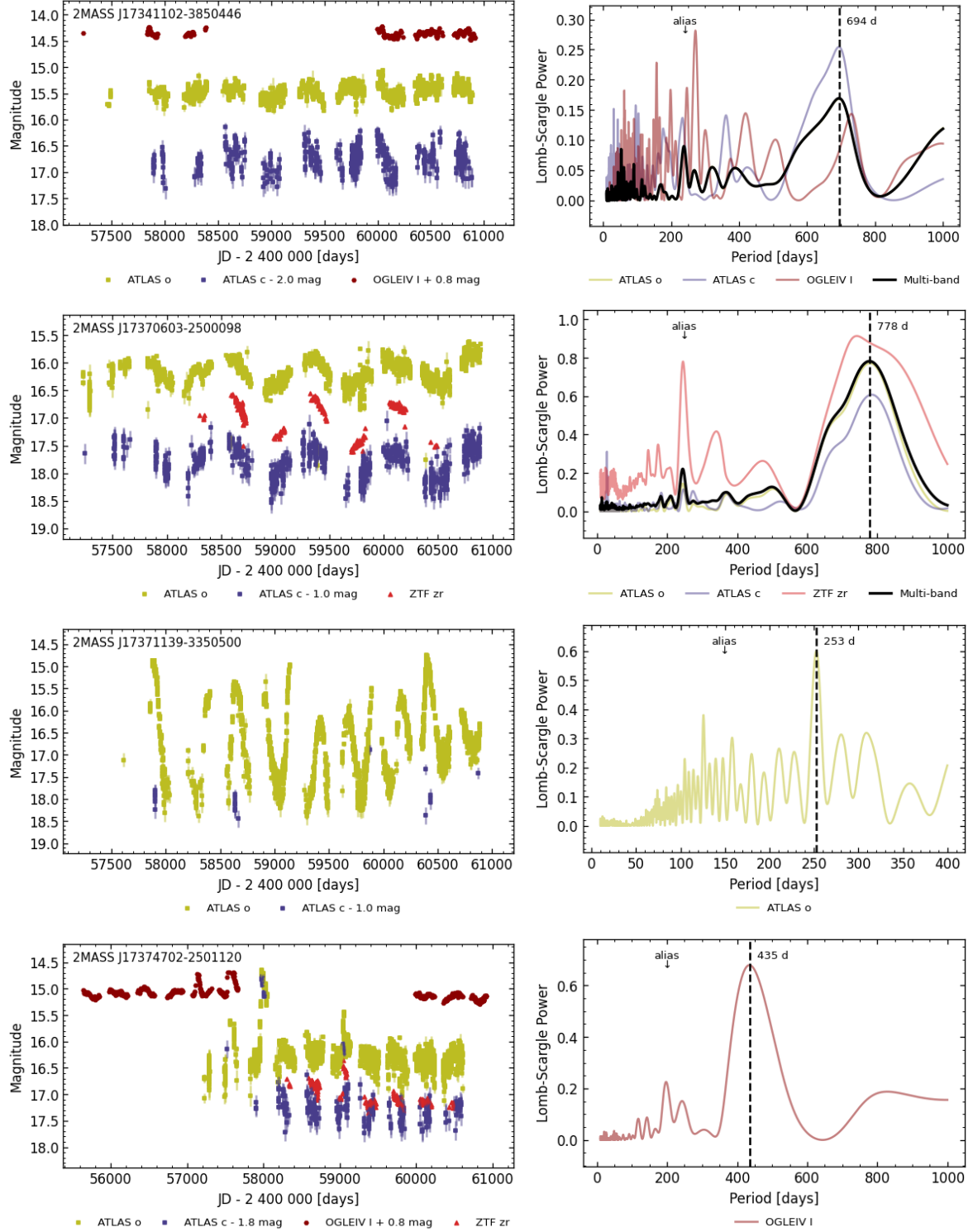


**Figure B1** – *continued* Light curves and Lomb–Scargle periodograms of the new symbiotic stars from this work.

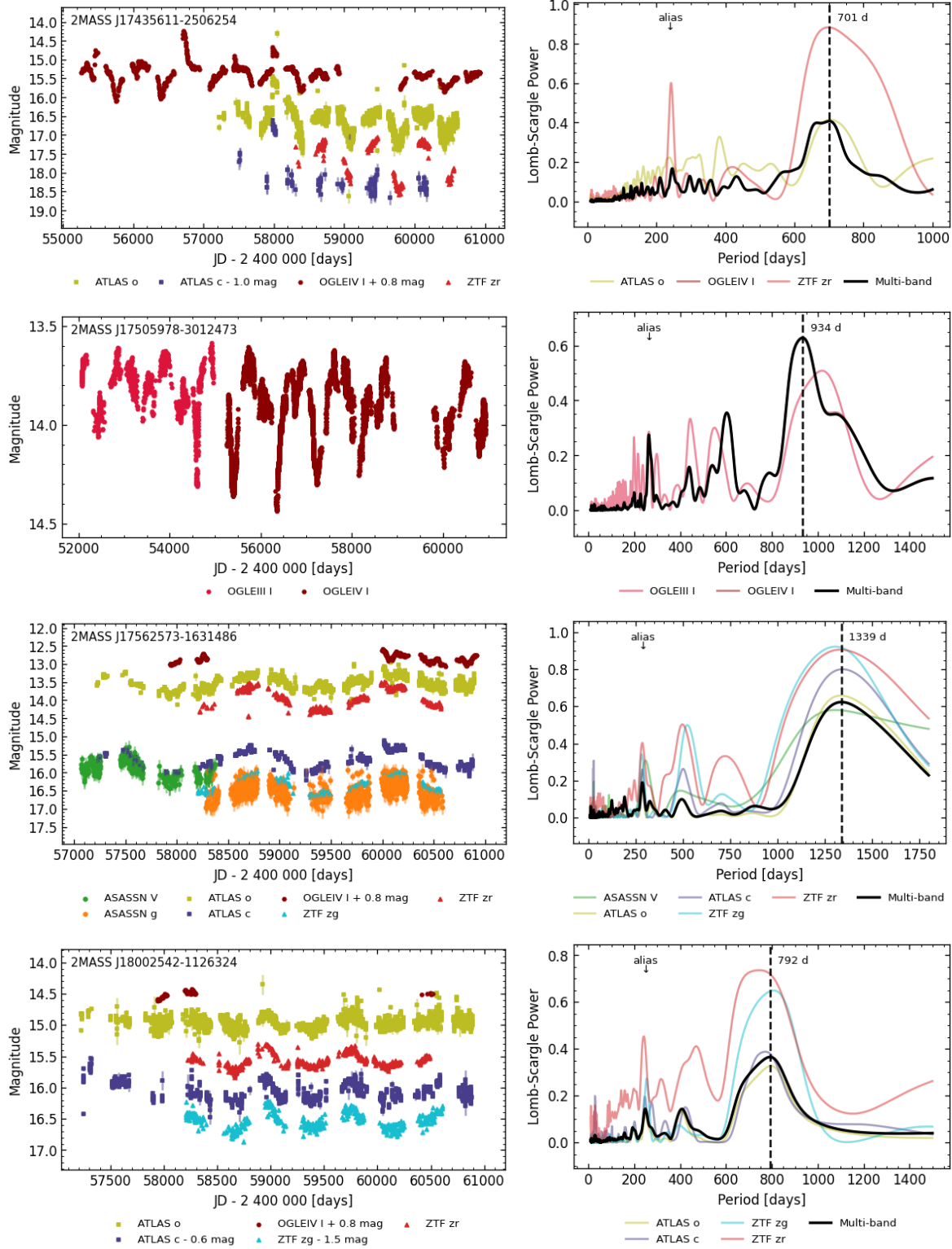


**Figure B1** – *continued* Light curves and Lomb–Scargle periodograms of the new symbiotic stars from this work.



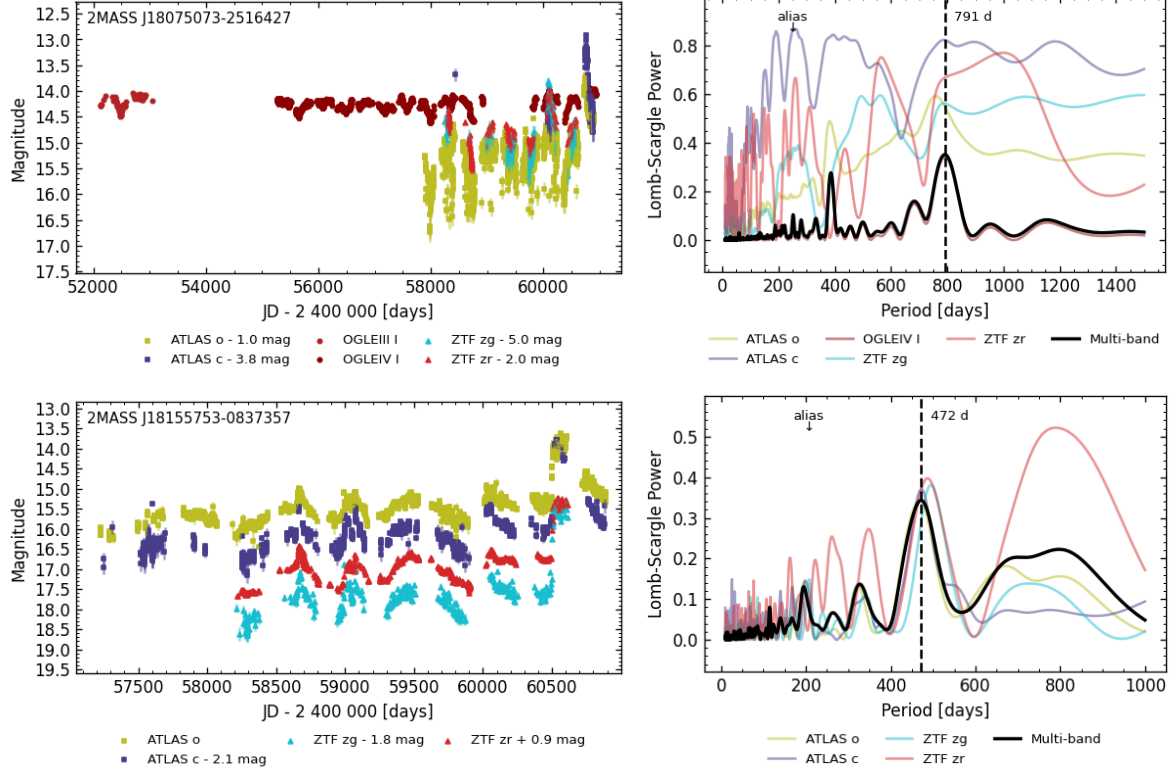


**Figure B1** – *continued* Light curves and Lomb–Scargle periodograms of the new symbiotic stars from this work.

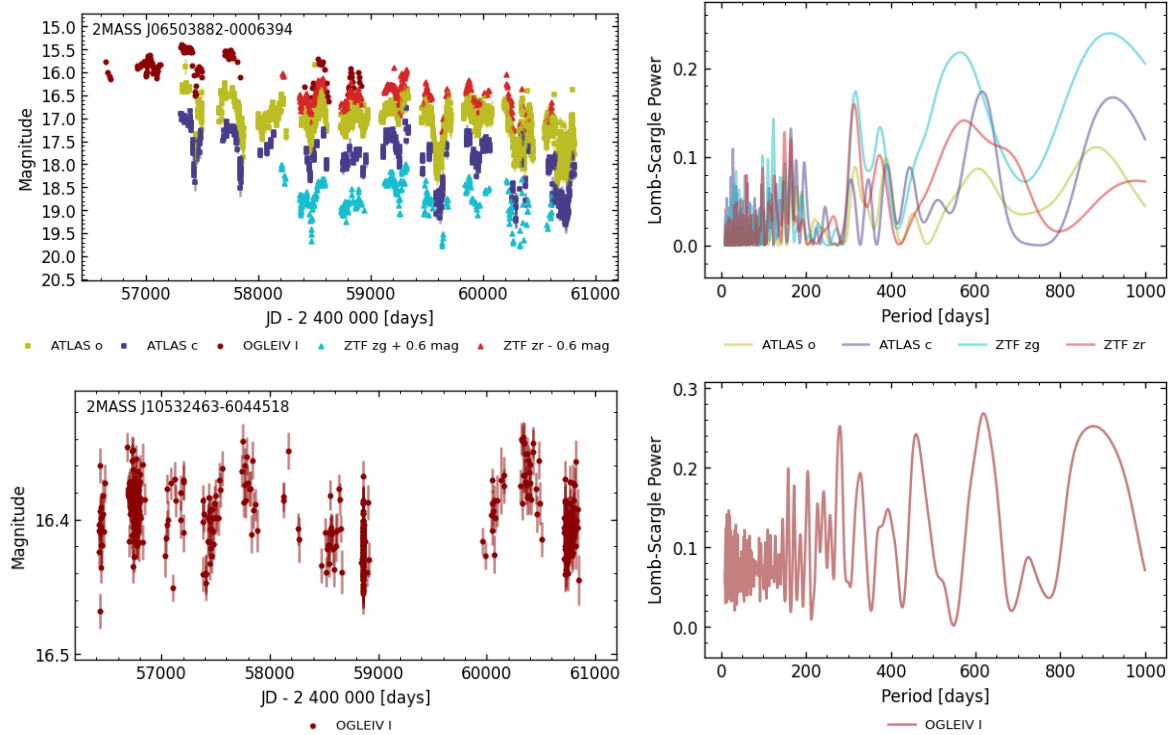


**Figure B2.** Light curves and Lomb–Scargle periodograms of the possible symbiotic stars from this work.

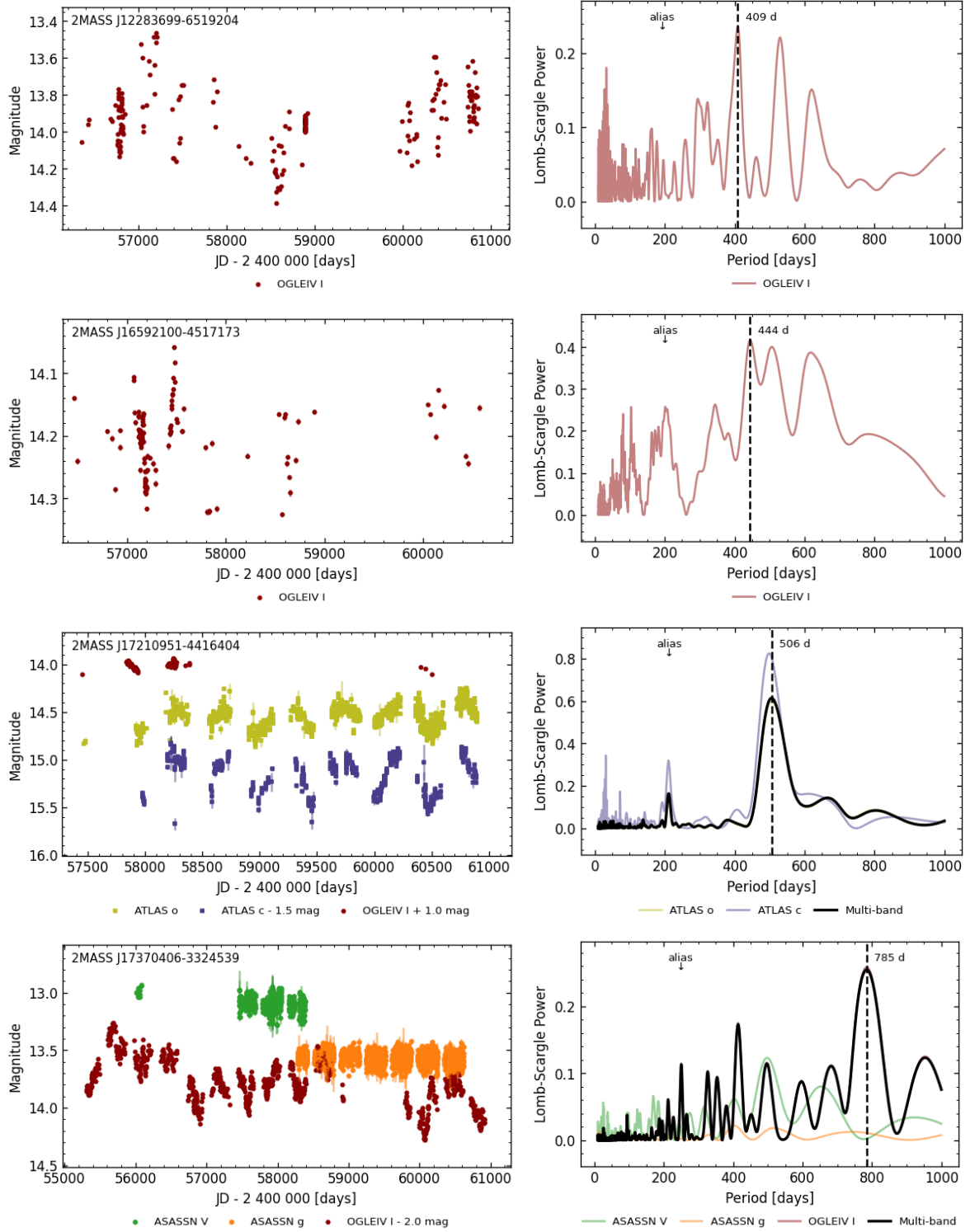


**Figure B2** – *continued* Light curves and Lomb–Scargle periodograms of the possible symbiotic stars from this work.

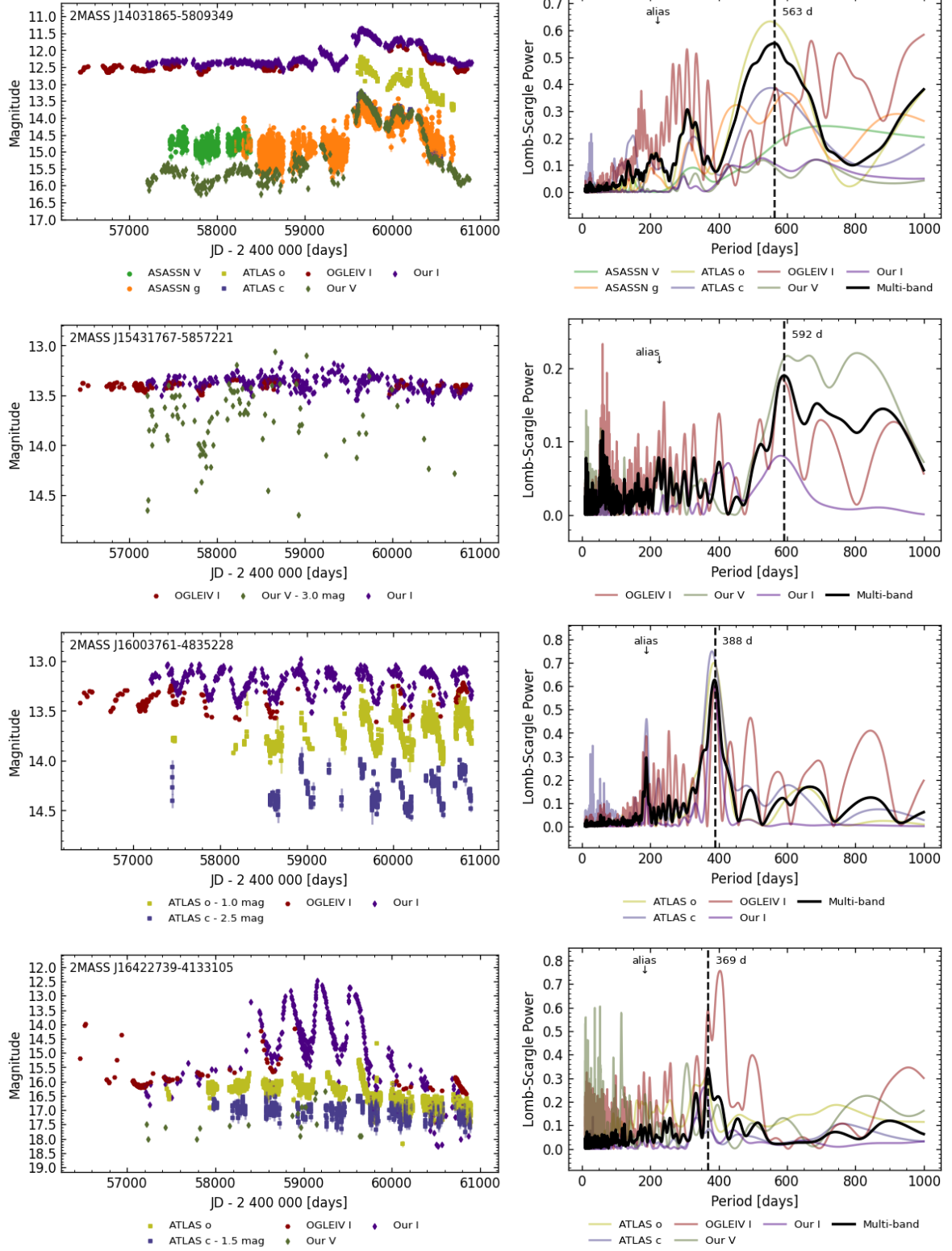


**Figure B3.** Light curves and Lomb–Scargle periodograms of the confirmed symbiotic stars from [Paper I](#).

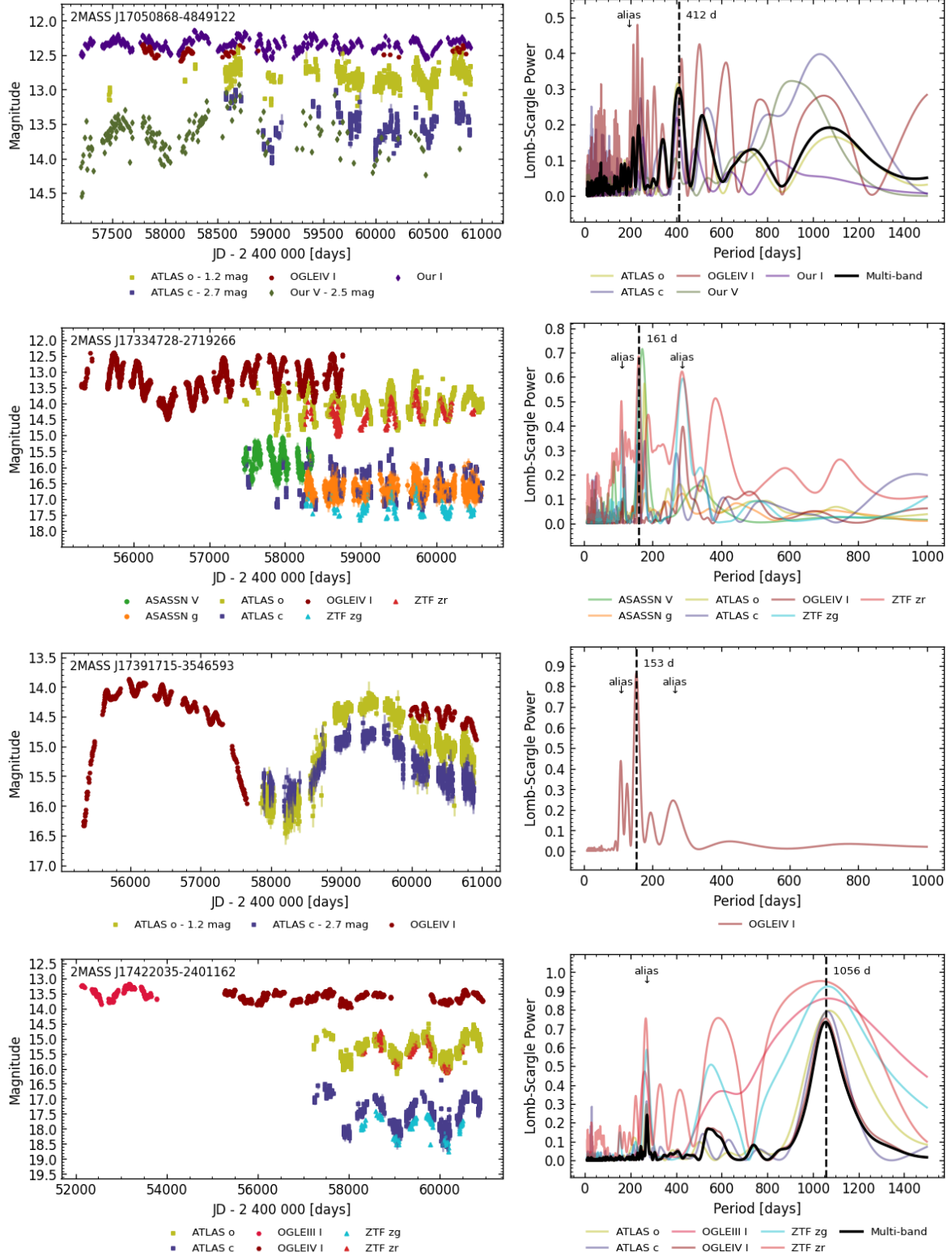


**Figure B3** – *continued* Light curves and Lomb–Scargle periodograms of the confirmed symbiotic stars from [Paper I](#).

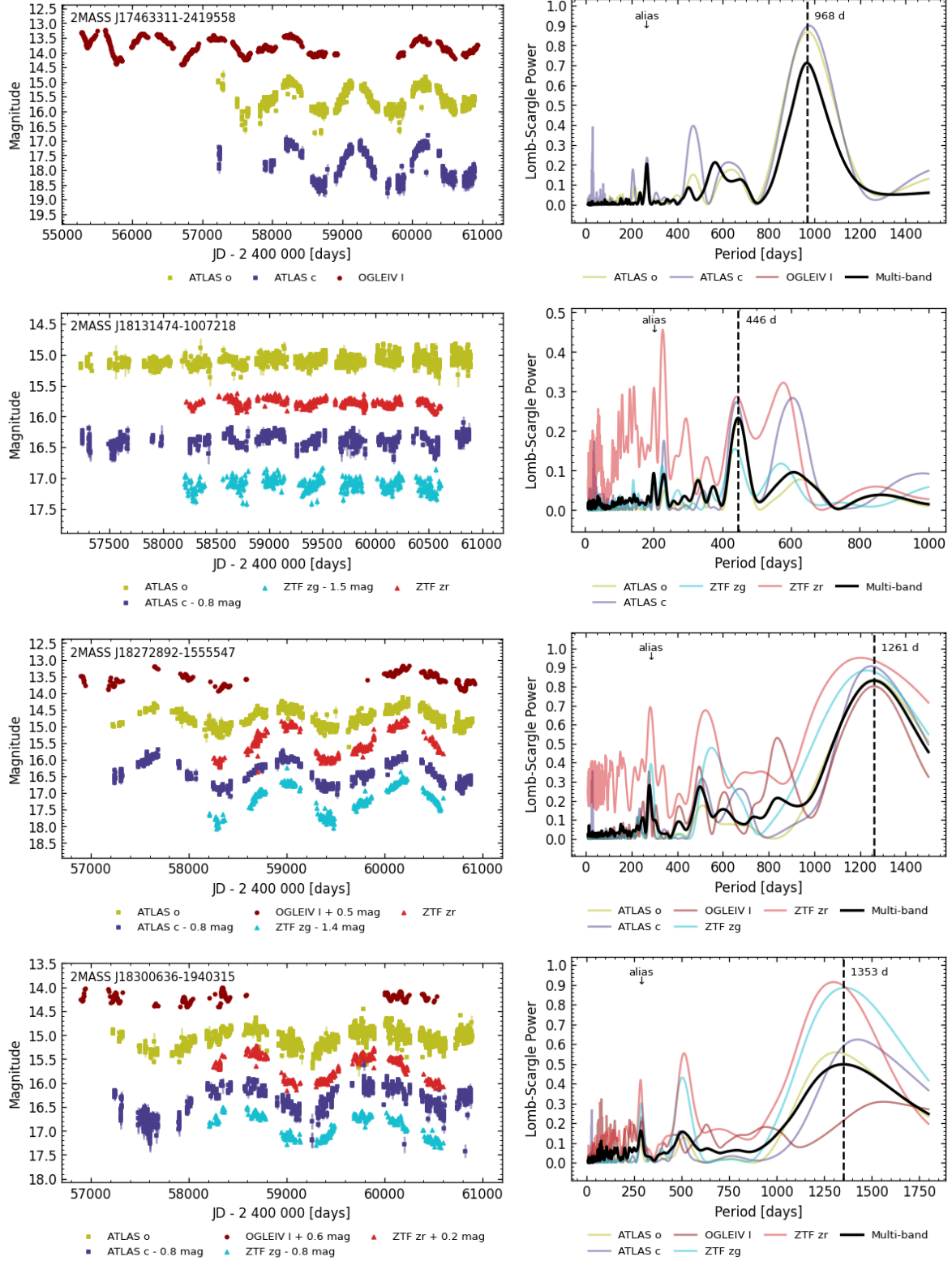


**Figure B3** – *continued* Light curves and Lomb–Scargle periodograms of the confirmed symbiotic stars from [Paper I](#).



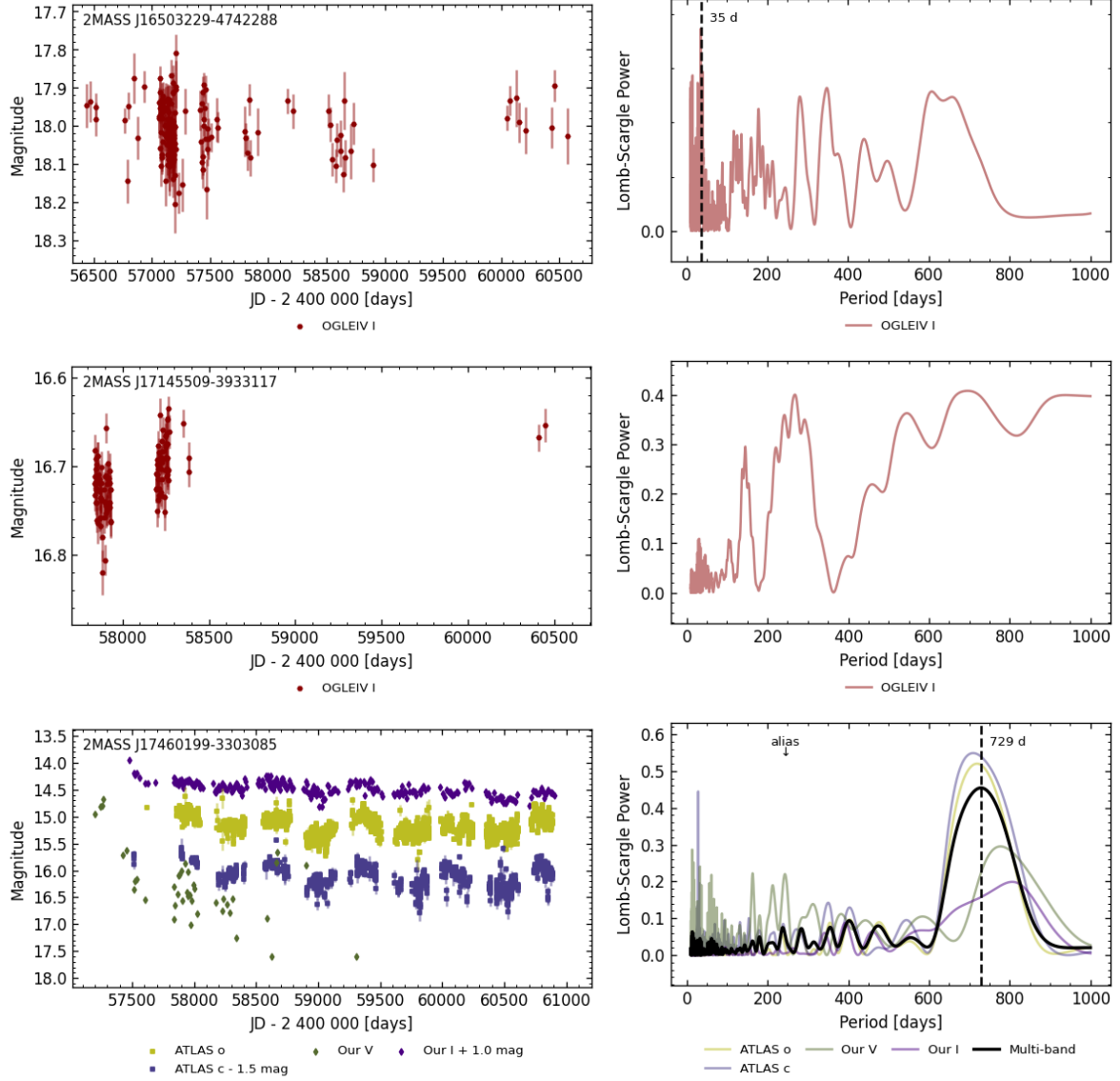


**Figure B4.** Light curves and Lomb-Scargle periodograms of the possible symbiotic stars from [Paper I](#).